Oxidative Reactivity of (N2S2)Pd(R)(X) Complexes (R = Me, Cl; X = Me, Cl, Br): Involvement of Pd(III) and Pd(IV) Intermediates

Jia Luo,[†] Nigam P. Rath[‡] and Liviu M. Mirica*[†]

[†]*Department of Chemistry, Washington University, St. Louis, Missouri, 63130-4899*

[‡]*Department of Chemistry and Biochemistry, University of Missouri – St. Louis, St. Louis, Missouri, 63121-4400*

**E-mail: mirica@wustl.edu*

Supporting information

Table of Contents

I. Cyclic voltammograms of (N2S2)Pd complexes S2

II. ESI-mass spectroscopy studies of Pd(III) intermediates S6

III. EPR simulation of reaction mixtures of 3 with 1 equiv $AcFc^+$ S7

IV. Reactivity studies of (N2S2)Pd complexes S8

V. Mechanistic studies of oxidative reactivities of 2 / 3 with 1 equiv $AcFc^+$ S19

VI. Computational details of 1^+, $[(^{tBu}N4)Pd^{III}Me_2]^+$, and 4^+complexes S20

VII. ^{1}H NMR of (N2S2)Pd complexes S29

VIII. X-ray crystal structures determination of 1, $1^{2+}(PF_6)_2$ and 6-Cl S36

IX. Preliminary crystal structures of 3 and 7 S48

X. References S63

I. Cyclic voltammograms of (N2S2)Pd complexes

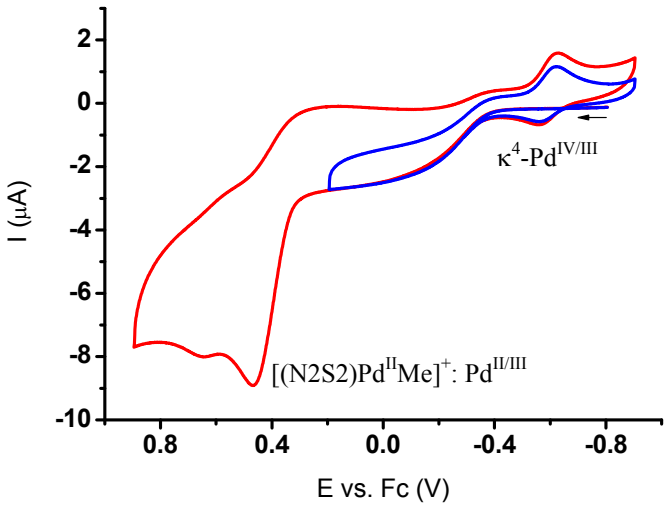

Figure S1. Cyclic voltammogram of 1.5 mM of (N2S2)$Pd^{II}Me_2$ (**1**) in 0.1 M Bu_4NClO_4/MeCN. Glassy carbon electrode, 500 mV/s scan rate.

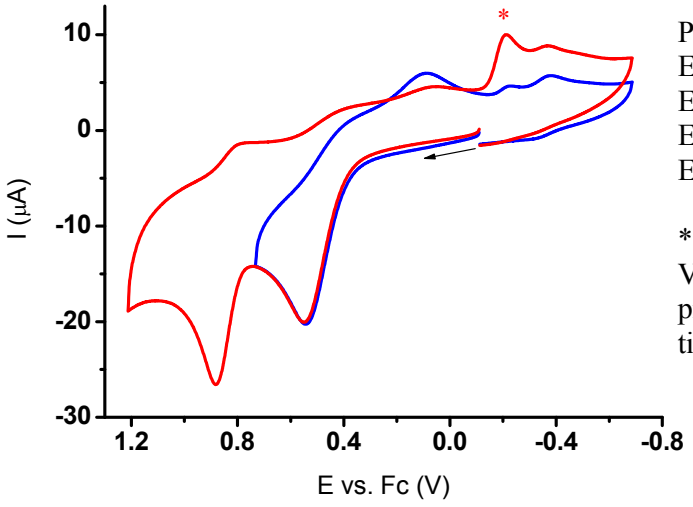

Potential vs Fc (V):
$E_{pa}^{II/III} = 0.55$
$E_{pc}^{III/II} = 0.09$
$E_{pa}^{III/IV} = 0.88$
$E_{pc}^{IV/III} = 0.80$

* The cathodic peak at -0.21 V comes from the side product produced during CV time scale.

Figure S2. Cyclic voltammogram of 1.0 mM of [(N2S2)$Pd^{II}Me]_2(OTf)_2$ (**5**) in 0.1 M Bu_4NBF_4/MeCN. Glassy carbon electrode, 100 mV/s scan rate.

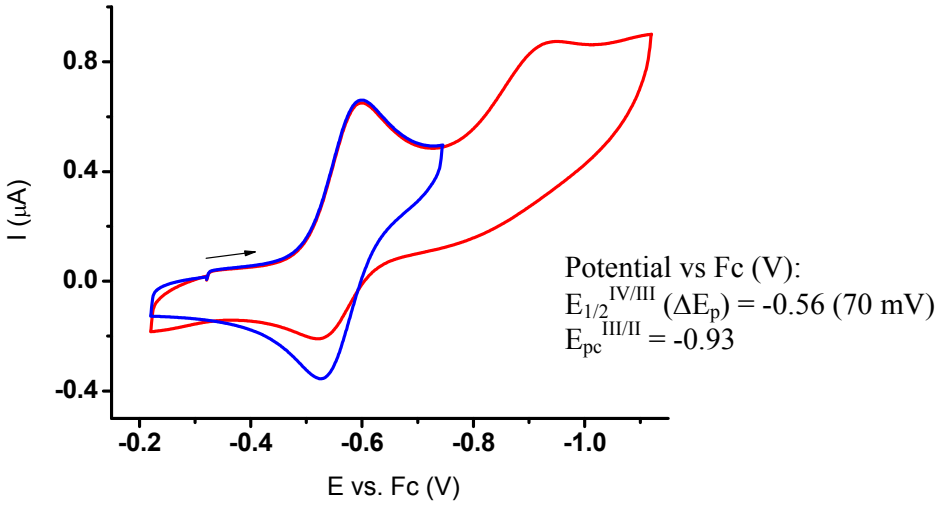

Figure S3. Cyclic voltammogram of 0.5 mM of $[(N2S2)Pd^{IV}Me_2](PF_6)_2$ ($\mathbf{1}^{2+}(PF_6)_2$) in 0.1 M Bu_4NClO_4/MeCN. Glassy carbon electrode, 100 mV/s scan rate.

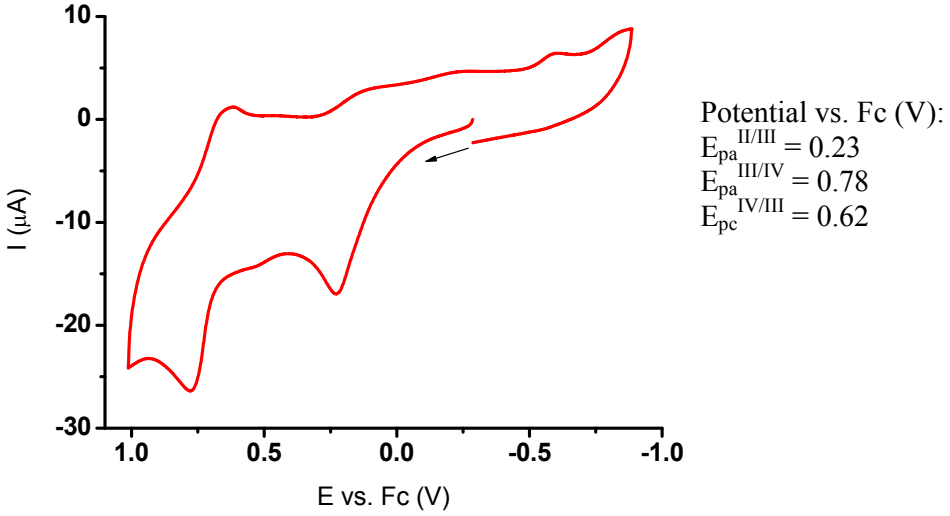

Figure S4. Cyclic voltammogram of 1.0 mM of $(N2S2)Pd^{II}MeCl$ (**2**) in 0.1 M Bu_4NClO_4/MeCN. Glassy carbon electrode, 100 mV/s scan rate.

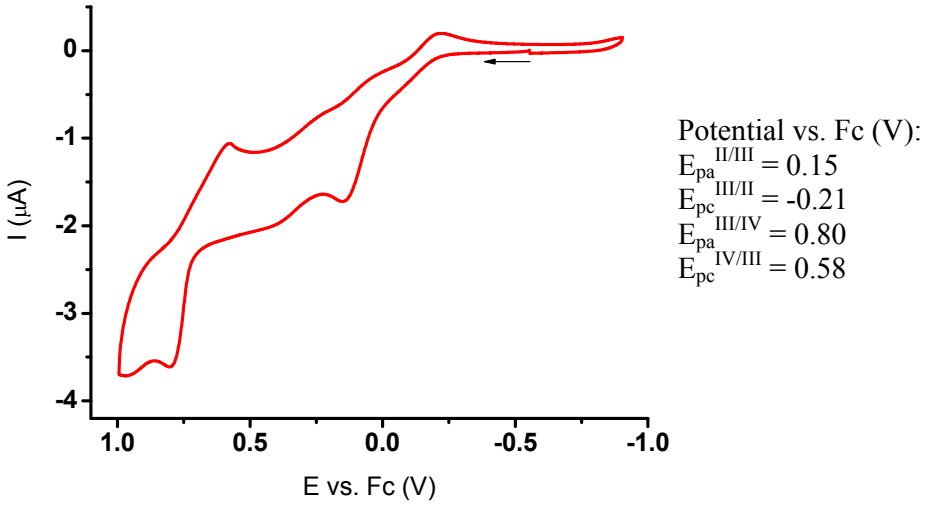

Figure S5. Cyclic voltammogram of 1.5 mM of (N2S2)Pd^{II}MeBr (**3**) in 0.1 M Bu_4NClO_4/MeCN. Glassy carbon electrode, 50 mV/s scan rate.

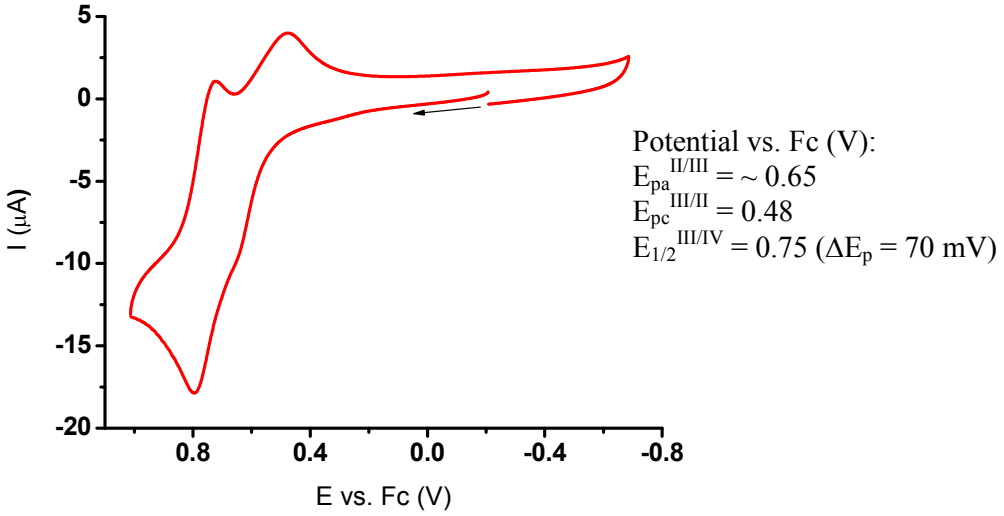

Figure S6. Cyclic voltammogram of 1.0 mM of (N2S2)$Pd^{II}Cl_2$ (**4**) in 0.1 M Bu_4NClO_4/MeCN. Glassy carbon electrode, 100 mV/s scan rate.

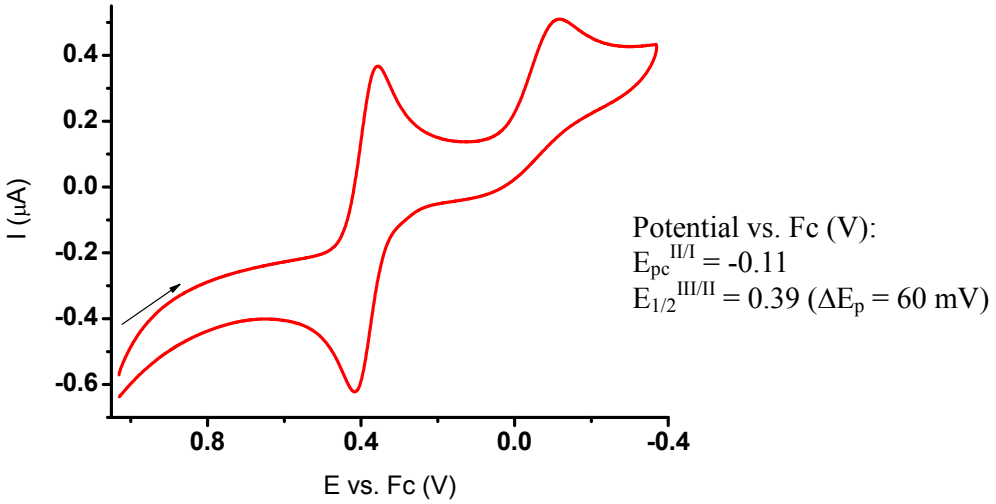

Figure S7. *In situ* cyclic voltammogram of -1e$^-$ electrolysis solution of 2.0 mM of **4** in 0.1 M Bu_4NClO_4/MeCN at -40 °C. Working electrode = platinum wire electrode, 100 mV/s scan rate. Reference electrode = Ag/AgCl wire.

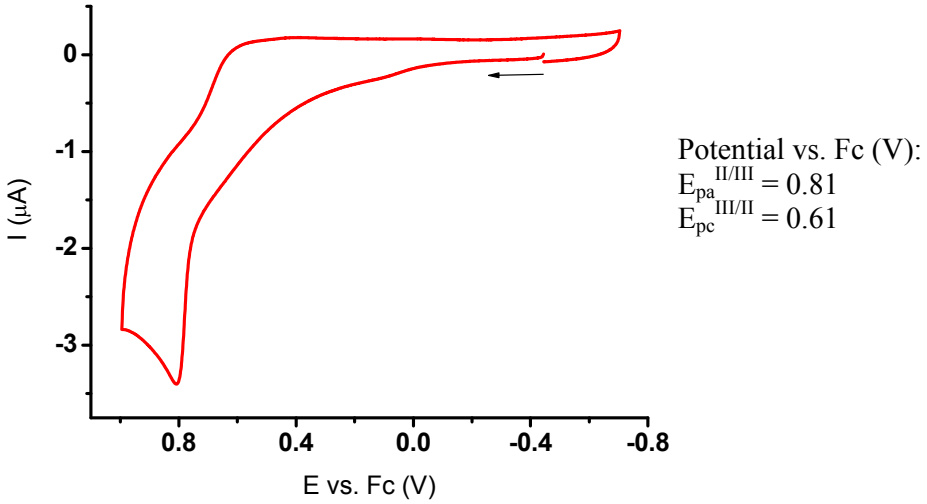

Figure S8. Cyclic voltammogram of 1.0 mM of [(N2S2)Pd^{II}Cl](OTf) (**6-Cl**) in 0.1 M Bu_4NClO_4/MeCN. Glassy carbon electrode, 100 mV/s scan rate.

II. ESI-mass spectroscopy studies of Pd(III) intermediates

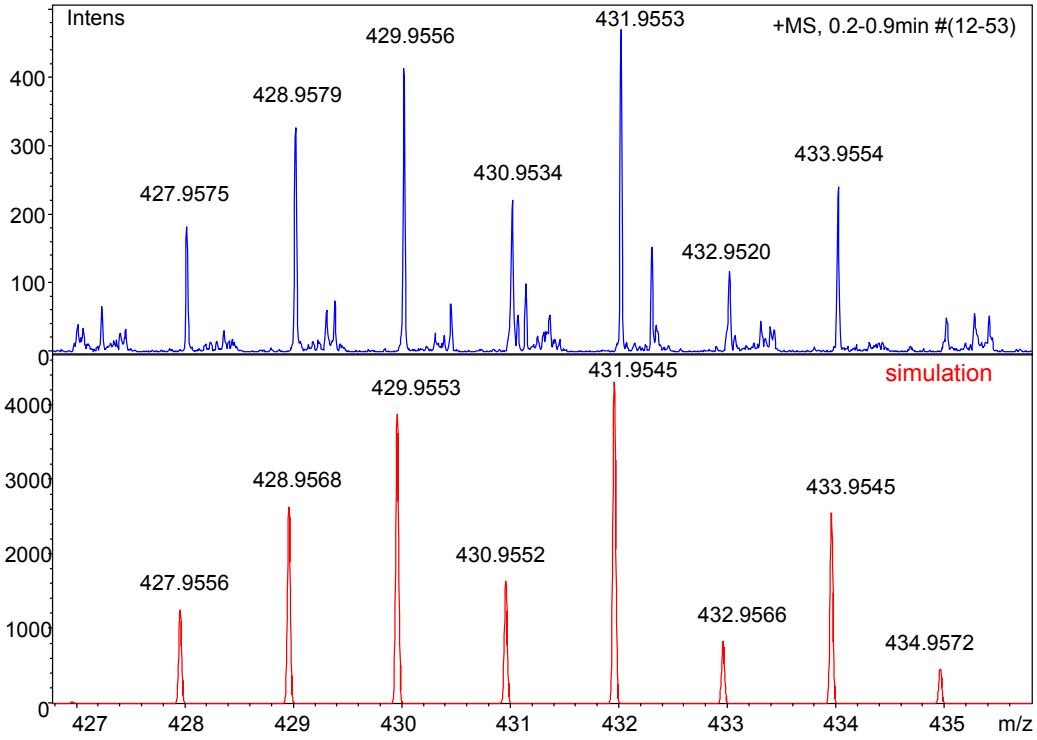

Figure S9. Top: ESI-MS of the reaction mixture of **2** and 1 eq. $AcFc^+$ in MeCN. Bottom: the enlarged peak at 429.9556 amu, and the simulation for $[(N2S2)Pd^{III}MeCl]^+$ ($\mathbf{2}^+$), 429.9553 amu.

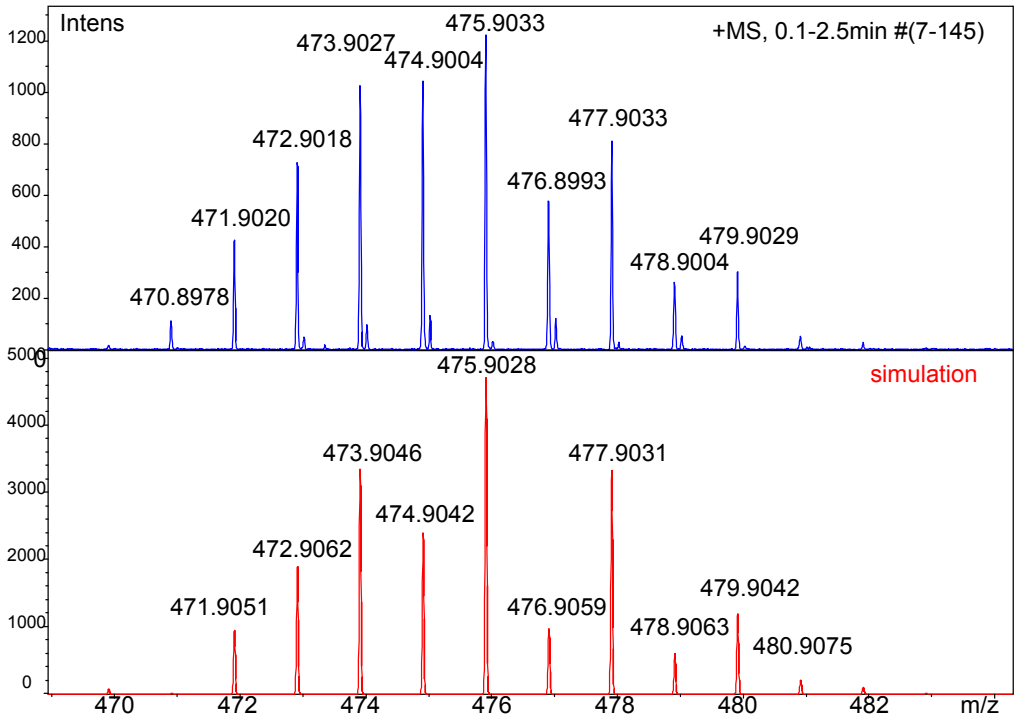

Figure S10. Top: ESI-MS of the reaction mixture of **3** and 1 eq. $AcFc^+$ in MeCN. Bottom: the enlarged peak at 473.9027 amu, and the simulation for $[(N2S2)Pd^{III}MeBr]^+$ ($\mathbf{3}^+$), 474.9046 amu.

III. EPR simulation of reaction mixtures of 3 with 1 equiv. $AcFc^+$

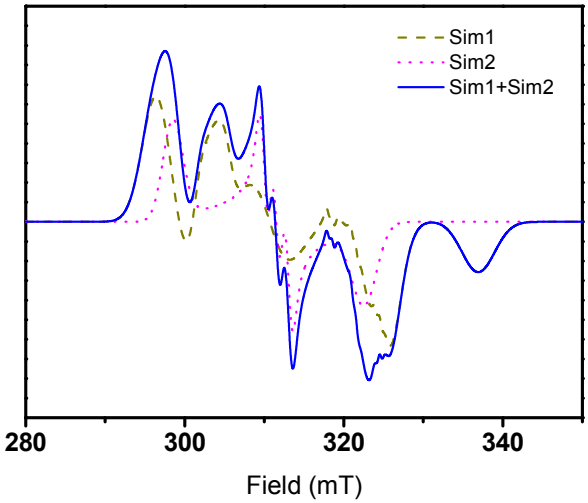

Figure S11. Simulation (blue) of EPR Spectrum of **3** + 1 equiv $AcFc^+$ by overlapping features of species A (yellow dashed) and species B (magenta dotted).

IV. Reactivity studies of (N2S2)Pd complexes

1) **1** + 1 eq. Fc^+ → **5** + MeMe

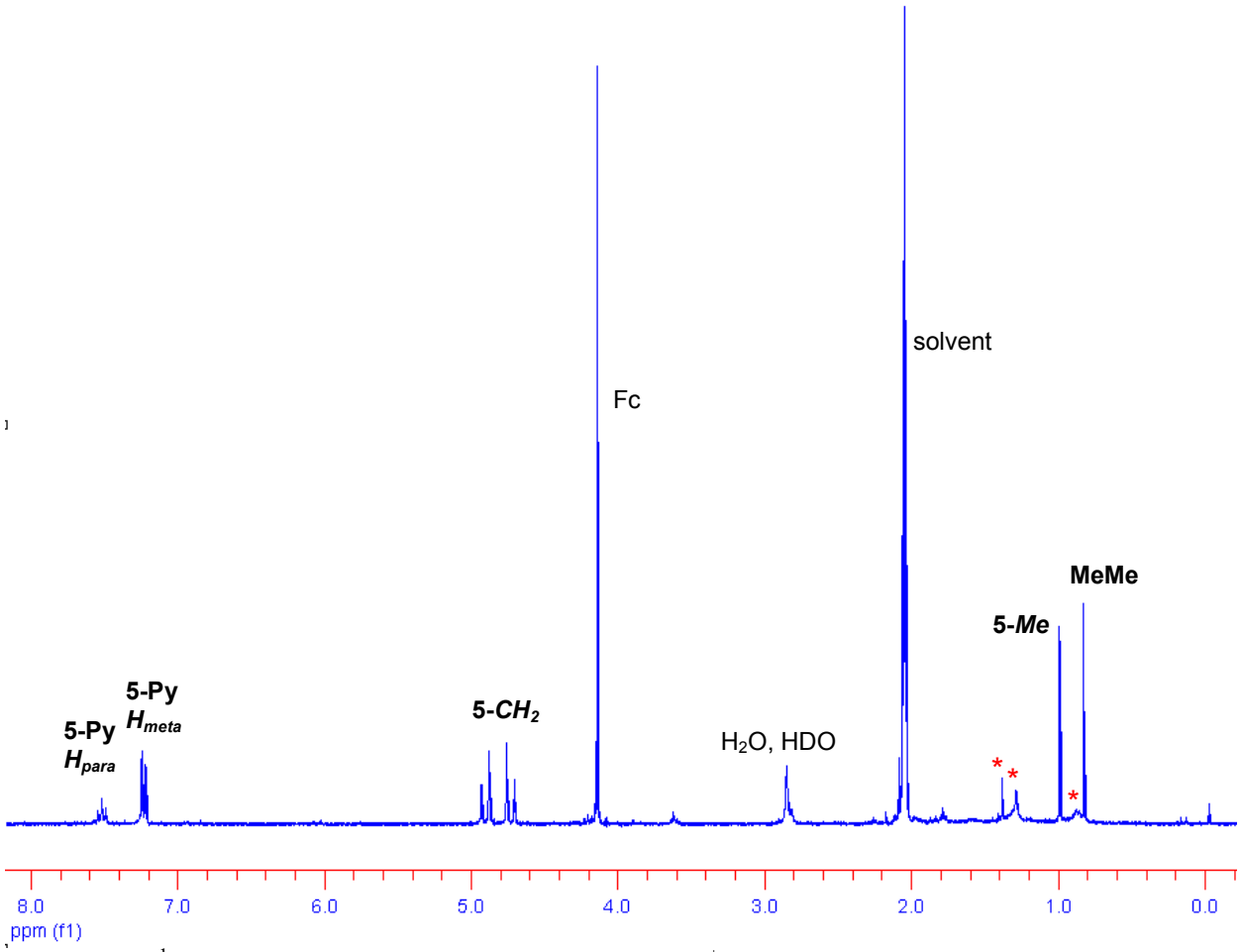

Figure S12. ^{1}H NMR reactivity study of **1** with 1 equiv Fc^+ in acetone-d_6. Peaks marked with asterisks are unidentified decomposition products that may contain Pd^{II}-Me group.

2) **1** + 1 eq. **1-*d₆*** + 2 eq. Fc^+ → **5** + **5-*d₃*** + CH_3CH_3 + CH_3CD_3 + [CD_3CD_3]

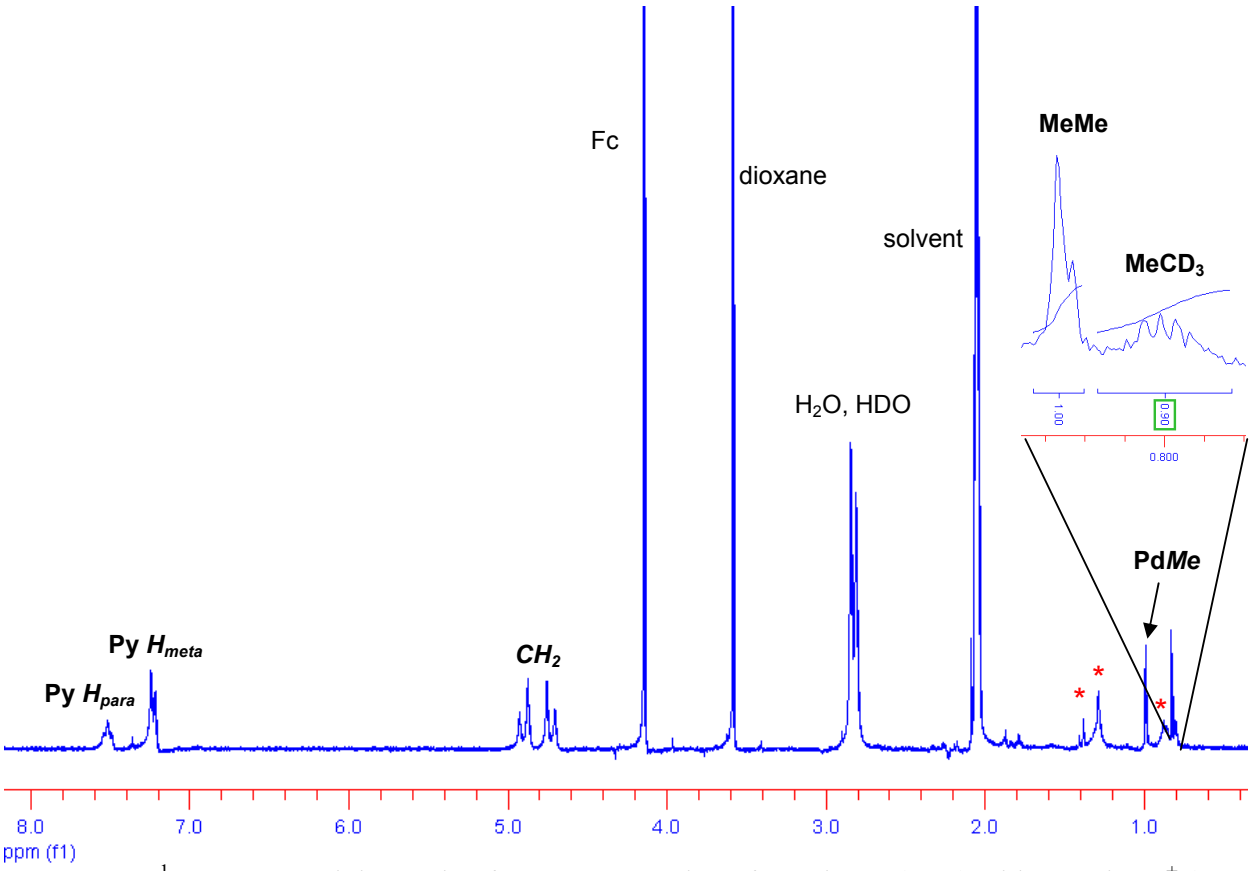

Figure S13. ^{1}H NMR reactivity study of crossover reaction of **1** and **1-*d₆*** (1 : 1) with 2 equiv Fc^+ (1 eq per Pd complex) in acetone-d_6. Assigned complexes peaks are from products of **5** and **5-*d₃***. Peaks marked with asterisks are unidentified decomposition products that may contain Pd^{II}-Me group.

3) **1** + 10 eq. MeI → MeMe + (N2S2)Pd^{II}MeI + N2S2

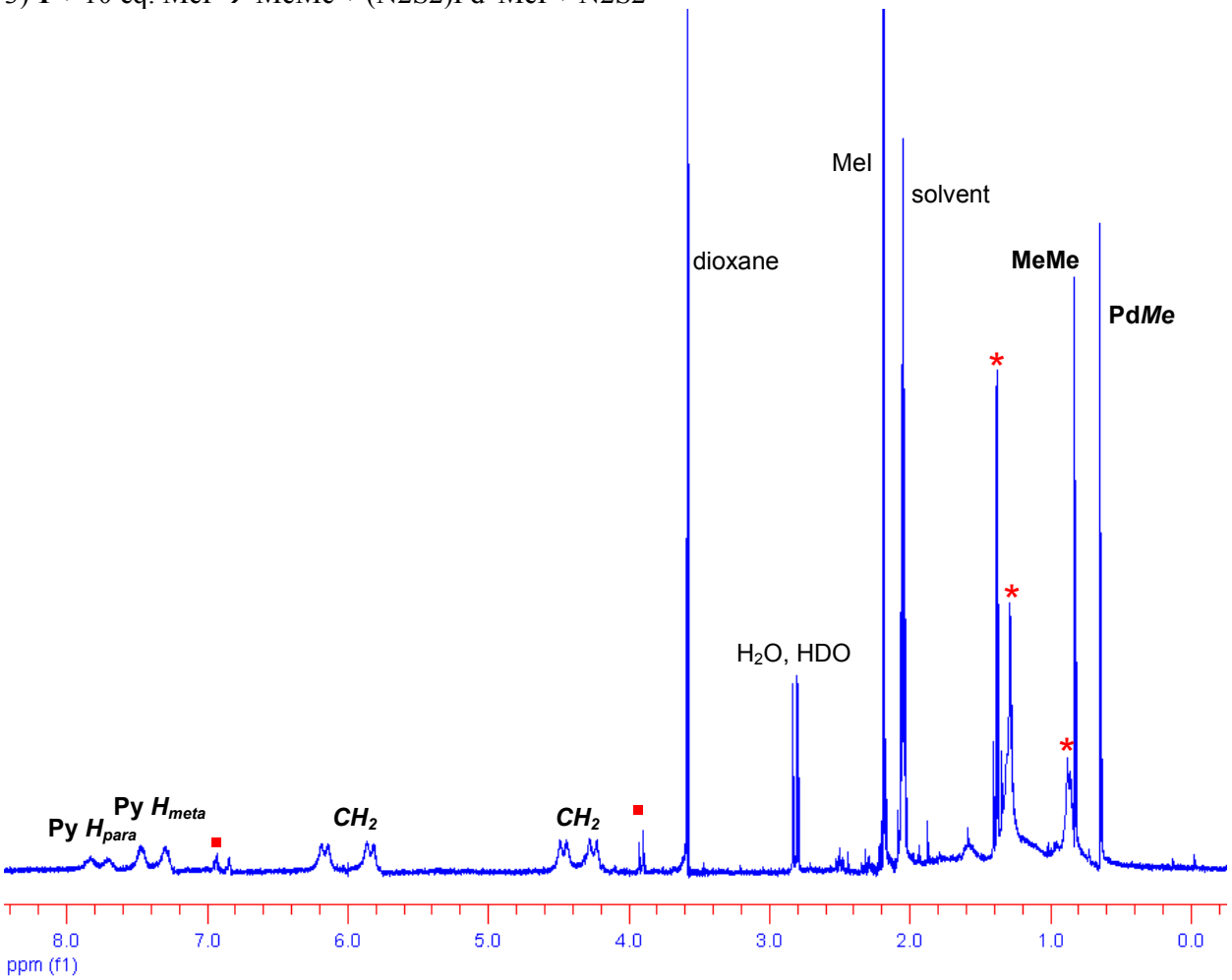

Figure S14. ^{1}H NMR reactivity study of **1** with 10 equiv MeI in acetone-d_6. Assigned peaks are for (N2S2)Pd^{II}MeI. Peaks marked with squares are from the free ligand N2S2; peaks marked with asterisks are unidentified decomposition products that may contain Pd^{II}-Me group.

4) **1** + 10 eq. CD_3I → CH_3CH_3 + CH_3CD_3 + (N2S2)Pd^{II}MeI + (N2S2)$Pd^{II}(CD_3)$I

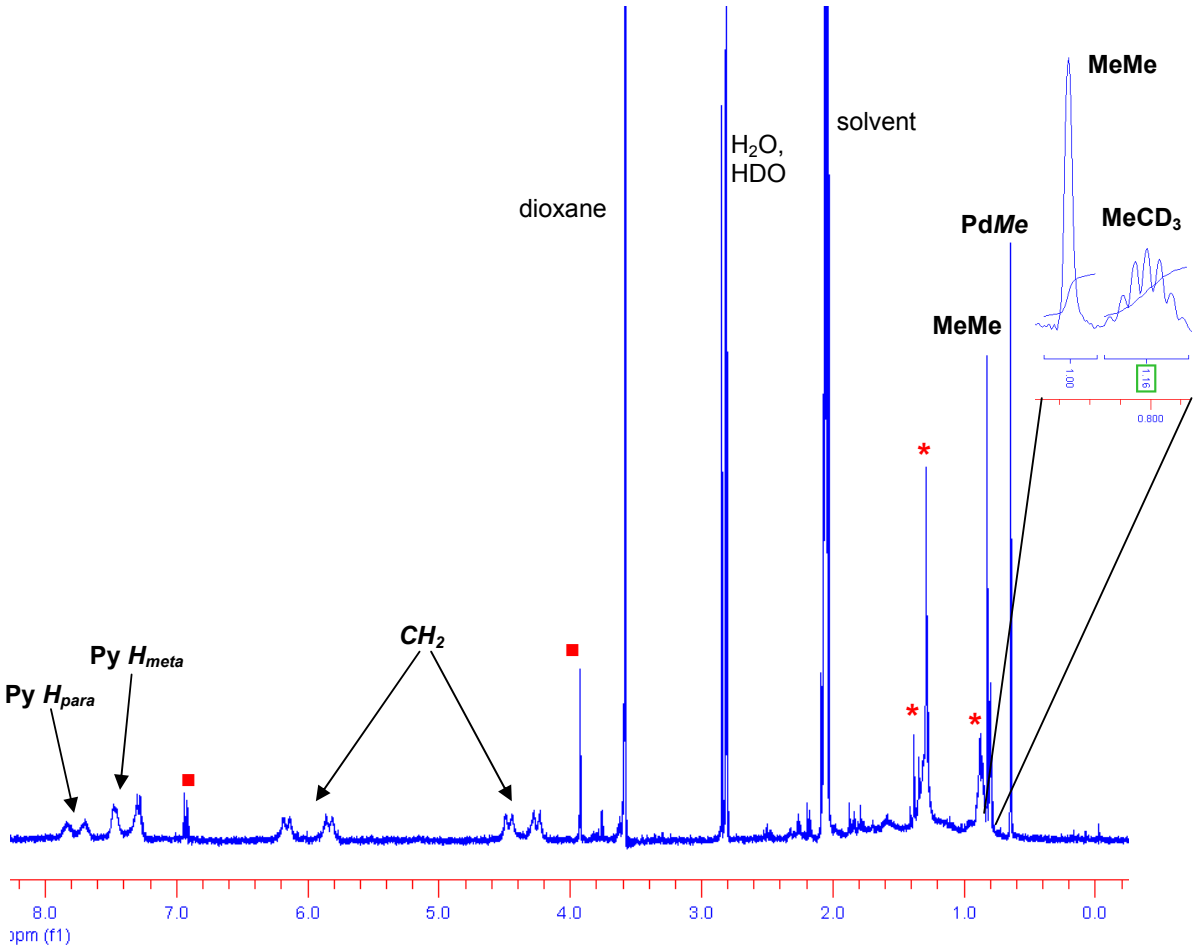

Figure S15. ^{1}H NMR reactivity study of **1** with 10 equiv CD_3I in acetone-d_6. Assigned peaks are for (N2S2)Pd^{II}MeI and (N2S2)$Pd^{II}(CD_3)$I. Peaks marked with squares are from the free ligand N2S2; peaks marked with asterisks are unidentified decomposition products that may contain Pd^{II}-Me group.

5) $\mathbf{1}^{2+}$ + 1.1 eq. $Co^{II}Cp_2$ → **5** + MeMe

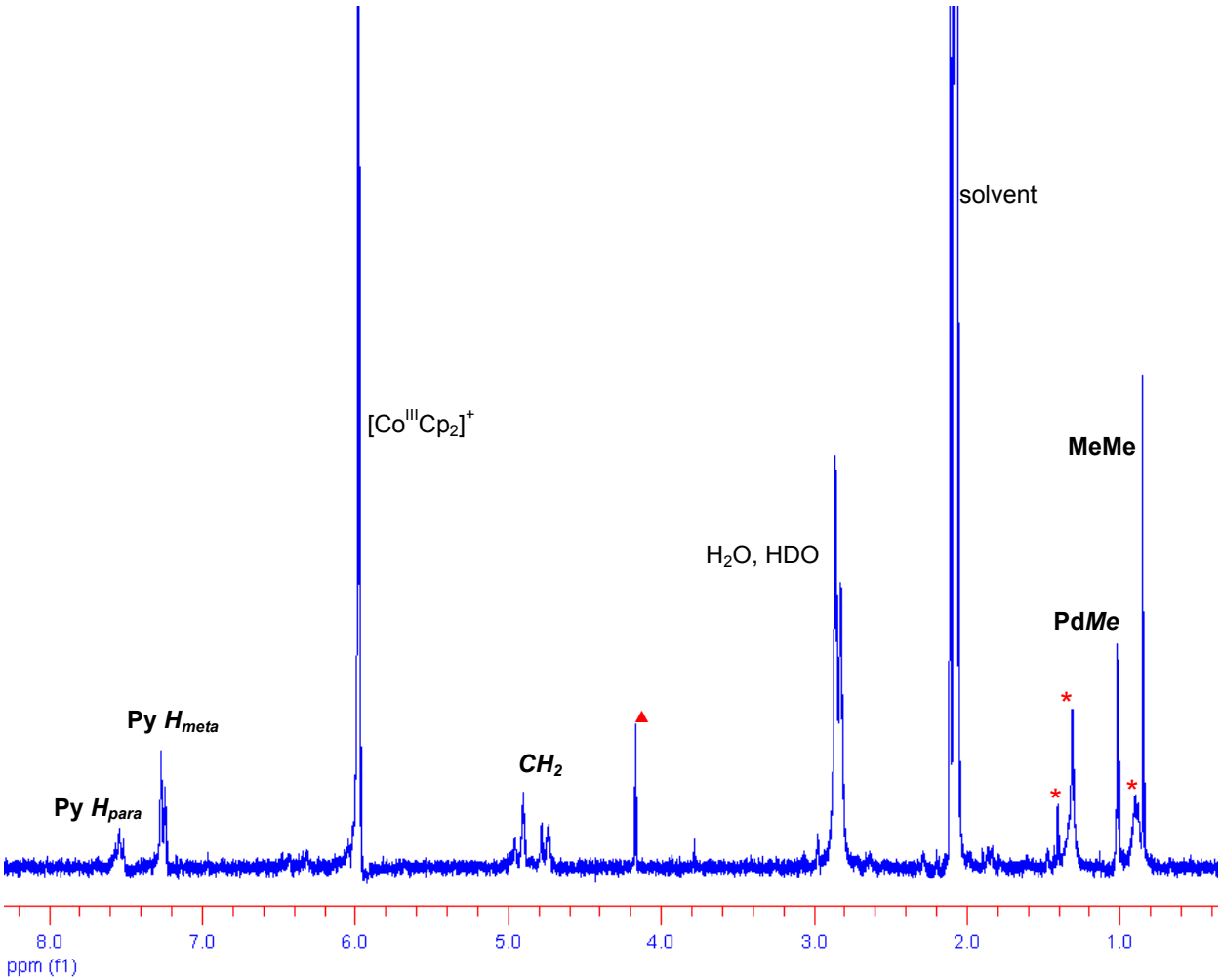

Figure S16. ^{1}H NMR reactivity study of $\mathbf{1}^{2+}$ with 1.1 equiv $Co^{II}Cp_2$ in acetone-d_6. Assigned peaks are for **5**. Peaks marked with asterisks are unidentified decomposition products that may contain Pd^{II}-Me group. The peak marked with triangle is due to ferrocene, a side product from the synthesis of $\mathbf{1}^{2+}(PF_6^-)_2$.

6) **2** + 1 eq. Fc^+ → MeCl + $\mathbf{1}^{2+}$ + **4** + **5** + **6-Cl**

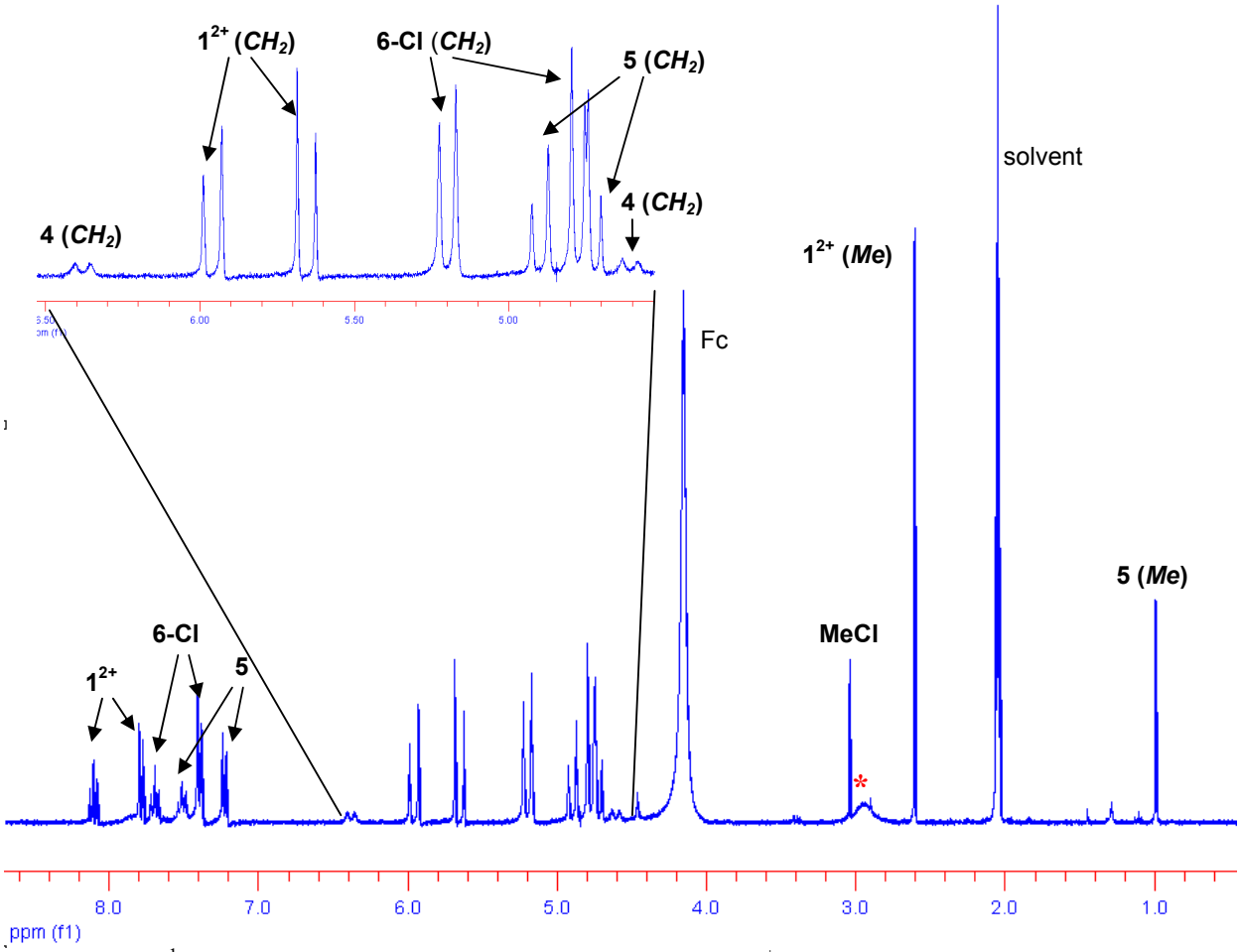

Figure S17. ^{1}H NMR reactivity study of **2** with 1 equiv Fc^+ in acetone-d_6. Peak marked with an asterisk is from trace amount of water.

Note: the reaction of **2** with 1 equiv $AcFc^+$ gives similar results.

7) **2** + $^{13}CH_3I$ → $^{13}CH_3Cl$ + (N2S2)Pd^{II}MeI

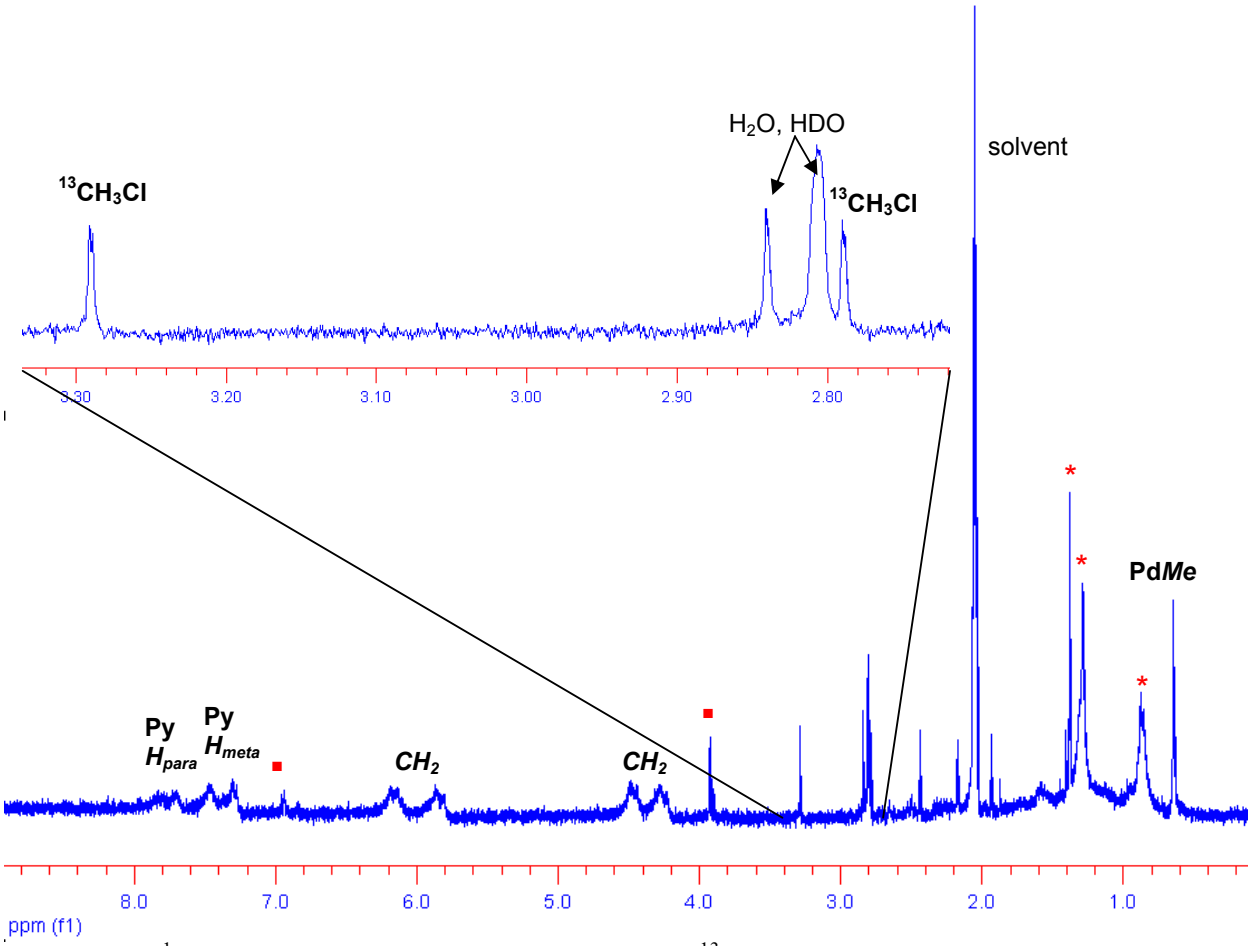

Figure S18. ^{1}H NMR reactivity study of **2** with 1 equiv $^{13}CH_3I$ in acetone-d_6. Assigned peaks are for (N2S2)Pd^{II}MeI. The peaks marked with squares are from the free ligand N2S2; peaks marked with asterisks are unidentified decomposition products that may contain Pd^{II}-Me group.

8) **3** + 1 eq. $AcFc^+$ → MeBr + **5** + **6-Br**

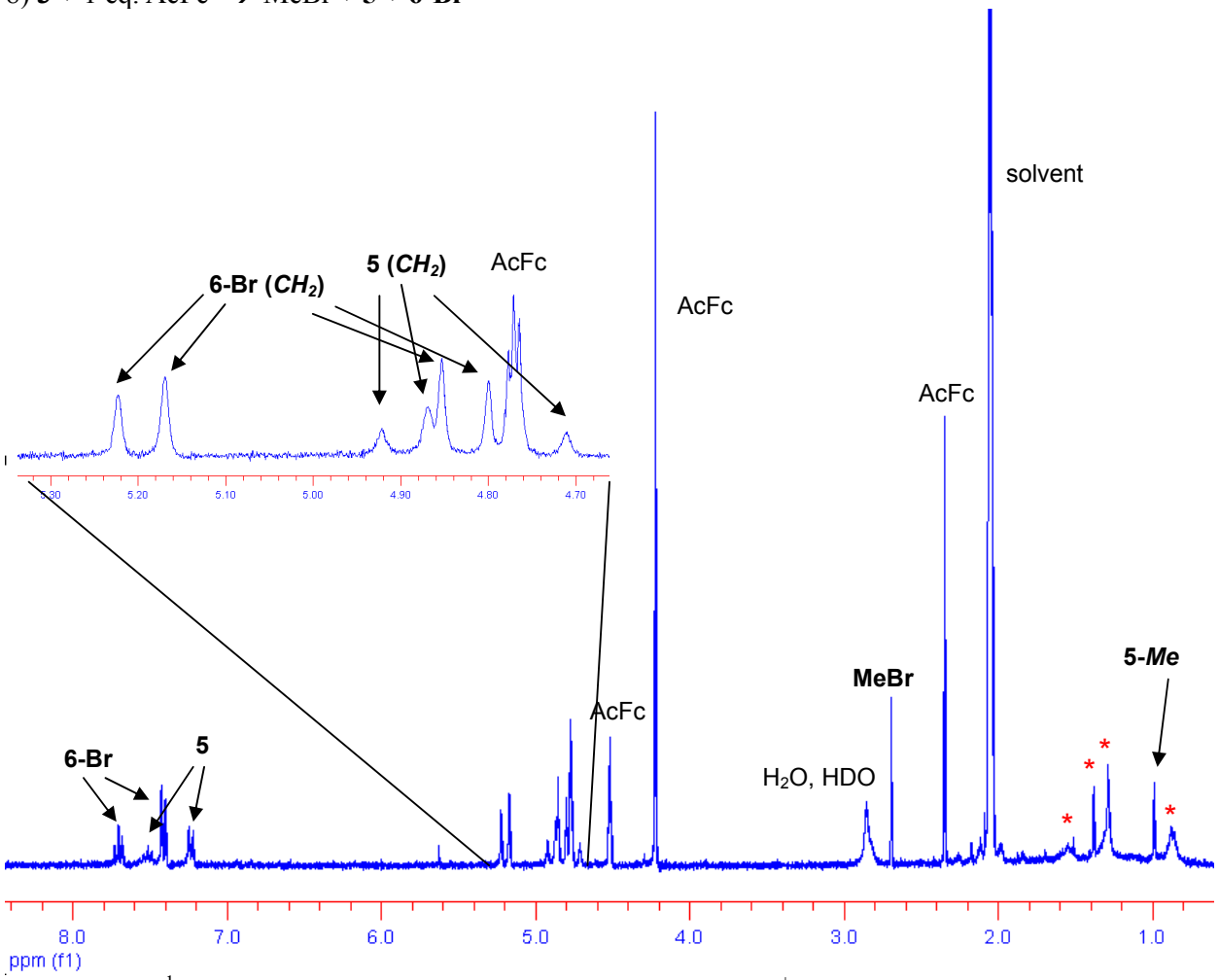

Figure S19. ^{1}H NMR reactivity study of **3** with 1 equiv $AcFc^+$ in acetone-d_6. Peaks marked with asterisks are unidentified decomposition products that may contain Pd^{II}-Me group.

9) **3** + $^{13}CH_3I$ → $^{13}CH_3Br$ + (N2S2)Pd^{II}MeI

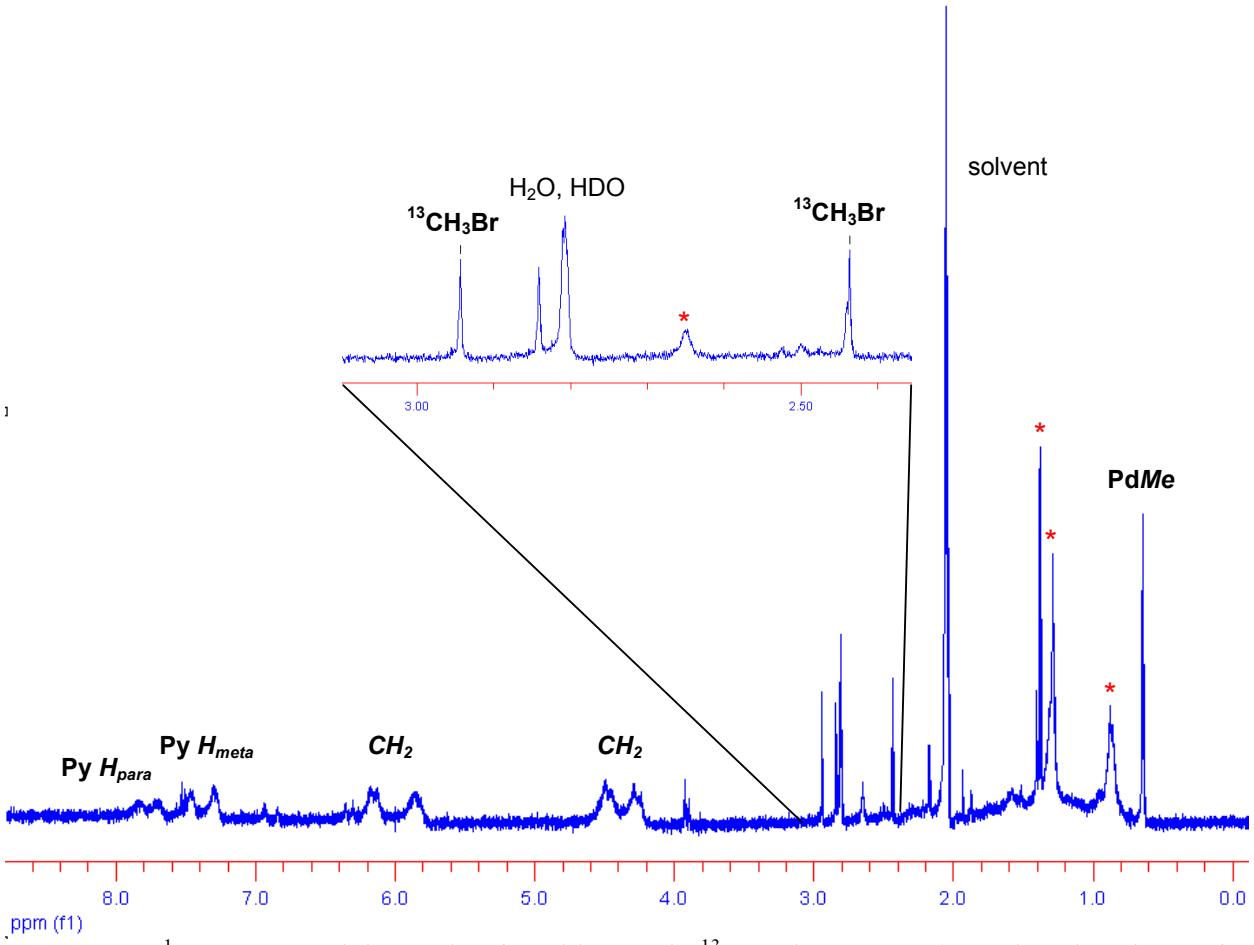

Figure S20. ^{1}H NMR reactivity study of **3** with 1 equiv $^{13}CH_3I$ in acetone-d_6. Assigned peaks are for (N2S2)Pd^{II}MeI. Peaks marked with asterisks are unidentified decomposition products that may contain Pd^{II}-Me group.

10) **2** + 1 eq. **3-^{13}C** + 2 eq. $AcFc^+$ → MeBr + $^{13}CH_3Br$ + **4** + **5** + **5-^{13}C** + **6-Cl/Br**

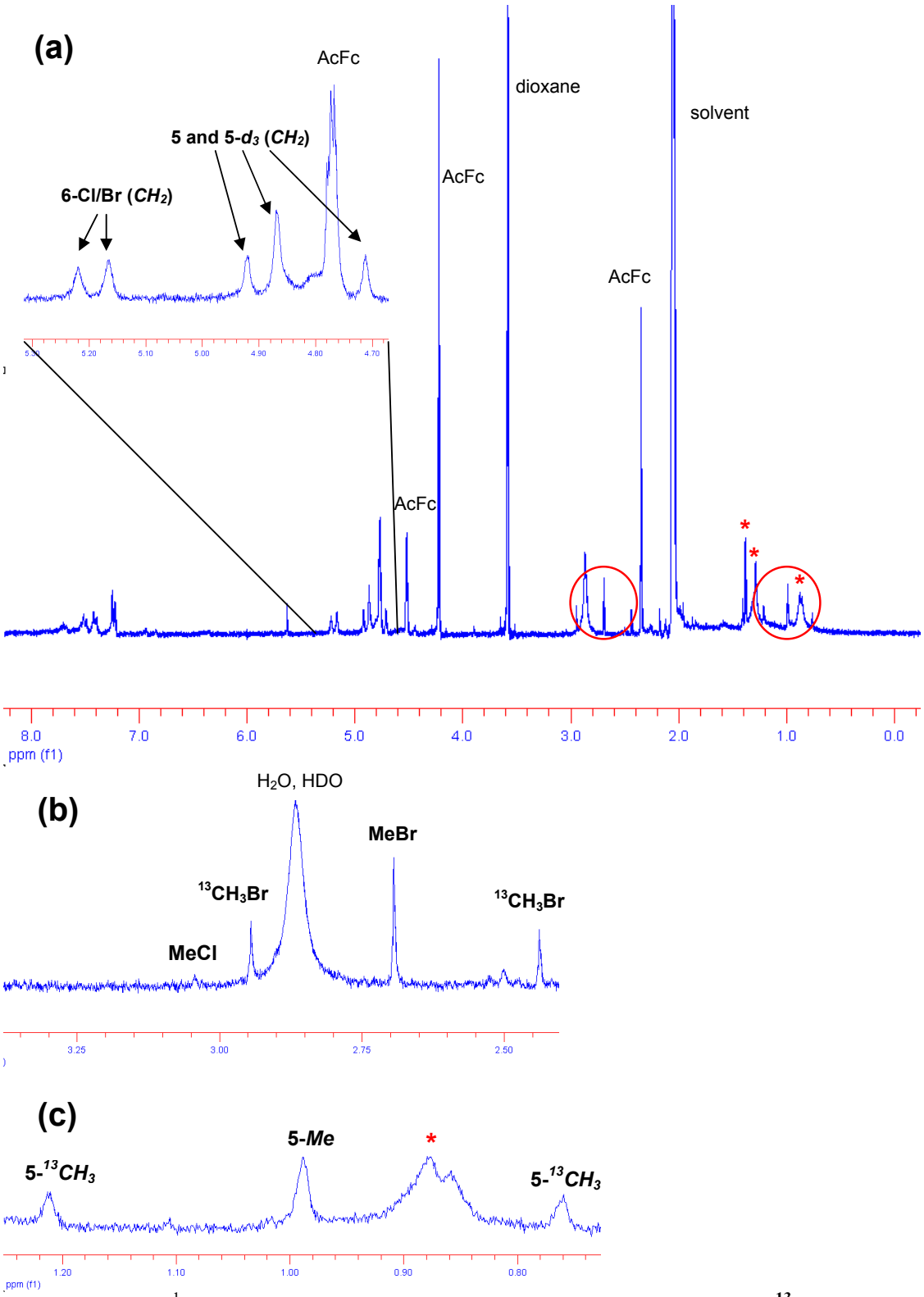

Figure S21. (a) ^{1}H NMR reactivity study of crossover reaction of **2** and **3-^{13}C** (1 : 1) with 2 equiv $AcFc^+$ (1 eq. per Pd complex) in acetone-d_6. (b) Enlarged region of 2.40 – 3.30 ppm. (c) Enlarged region of 0.72 – 1.26 ppm. Peaks marked with asterisks are unidentified decomposition products that may contain Pd^{II}-Me group.

11) $\mathbf{1}^{2+}$ + 1.8 eq. $Bu_4N^+Br^-$ → MeBr + **3**

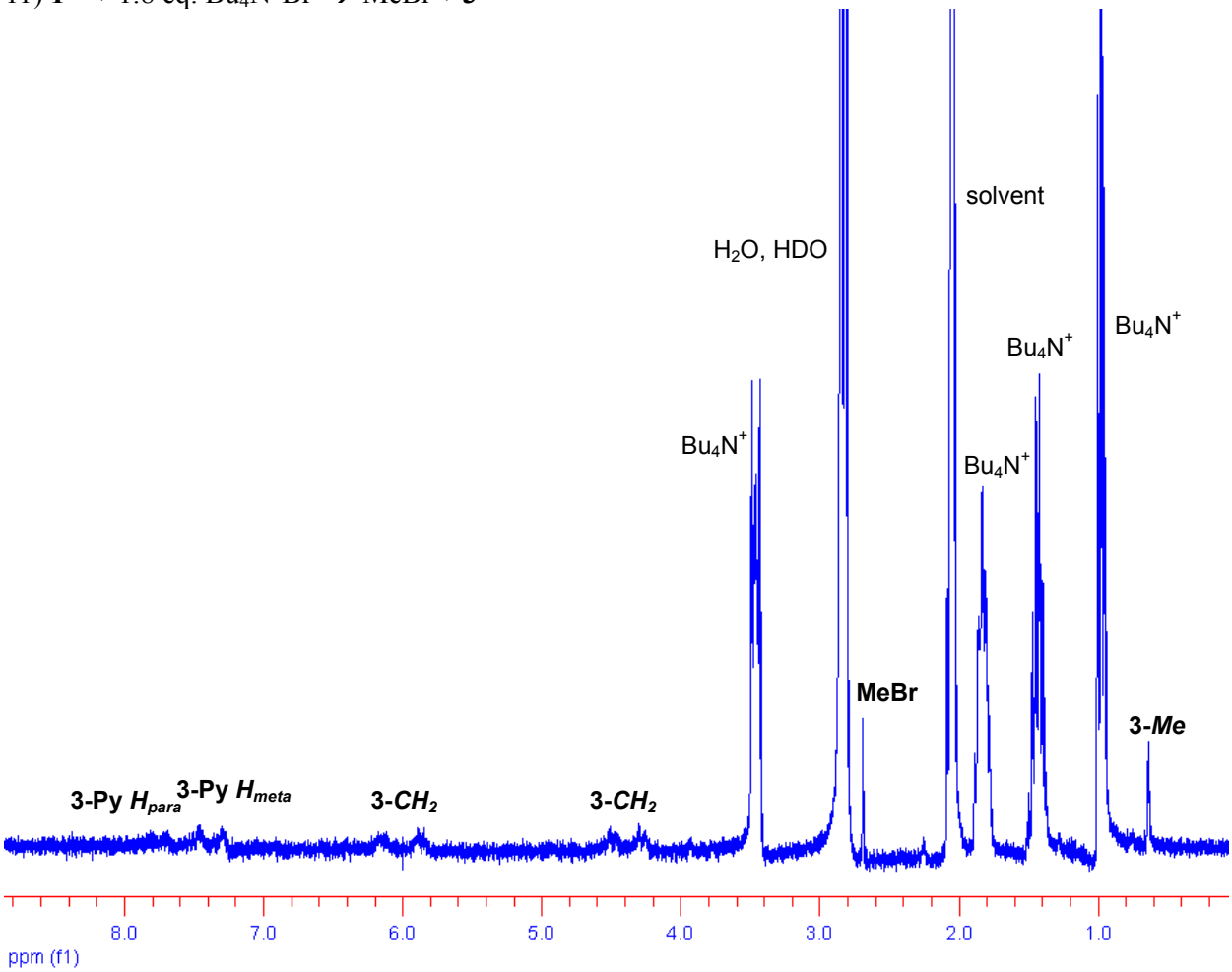

Figure S22. ^{1}H NMR reactivity study of $\mathbf{1}^{2+}$, 5 min after adding 1.8 equiv $Bu_4N^+Br^-$ in acetone-d_6.

V. Mechanistic studies of oxidative reactivities of 2 / 3 with 1 equiv. $AcFc^+$

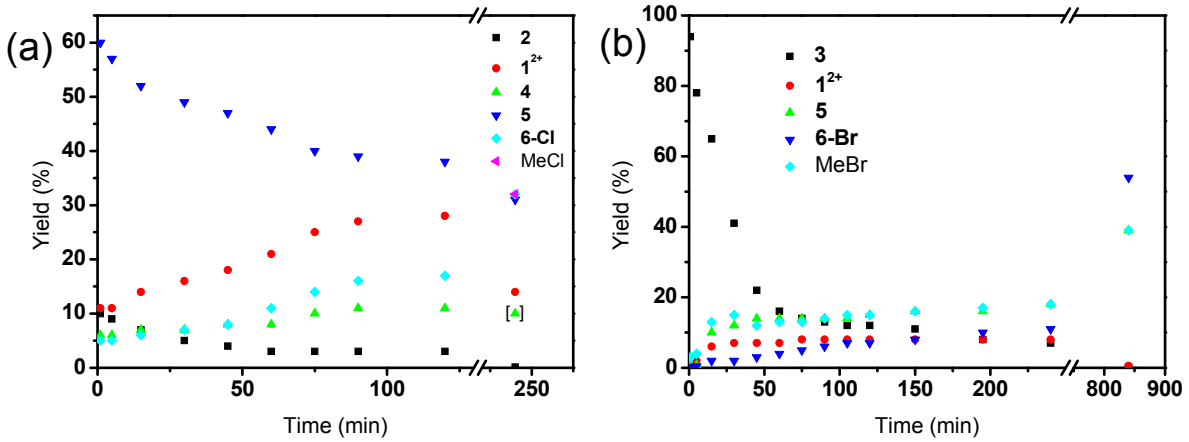

Figure S23. Time-dependent ^{1}H NMR studies of oxidation reaction of **2** (a) and **3** (b) with 1 equiv $AcFc^+$ in acetone-d_6 at -20 ºC, followed by monitoring at RT (the last data point in each graph corresponds to the final yield of the products at RT).

Note: For (a), the experiment in the first 2 hours was monitored at -20 ºC, followed by continued monitoring at RT for 4 hours. The H_2O peak overlaps with MeCl at -20 ºC, thus the amount of MeCl could be obtained only at RT. Since $(N2S2)Pd^{II}Cl_2$ (**4**) precipitates out of solution, the final yield of **4** is estimated as 100% - yields of other Pd products. For (b), the experiment in the first 4 hours was monitored at -20 ºC, followed by continued monitoring at RT up to 6 hours in total.

VI. Computational details

The density functional theory (DFT) calculations were performed with the program package Gaussian 09.[1] The B3LYP functional[2] along with the Stevens CEP-31G(d) valence basis sets and effective core potentials were employed.[3] The CEP-31G(d) valence basis set is valence triple-ζ for palladium and double-ζ for main group elements, with an additional *d* polarization function for Cl. This functional/ basis set combination has been shown previously to reproduce well experimental parameters of Pd complexes.[4] Single point calculations were performed on the geometry optimized coordinates of the cations of $\mathbf{1}^+$ and $\mathbf{4}^+$ with the N2S2 ligand adopting a κ^4 conformation. The ground state wavefunctions were investigated by analysis of the frontier MOs, and the atomic contributions to MO's were calculated using the program Chemissian (Tables S1-S3).[5] TD-DFT calculations were employed to obtain the predicted absorption bands and their major contribution transitions (Table S4). The calculated UV-vis spectrum was generated using GaussSum,[6] with a full width at half maximum (FWHM) value of 3,000 cm^{-1} (Figure S24).

Table S1. Isocontour plots and energies of selected molecular orbitals for **1**$^{+}$. The atomic simple contributions to the MOs are shown for the Pd atoms, the S atoms, the equatorial pyridine N atoms (N_{eq}), and the C atoms from the Me group. Balance contribution comes from ligand-based C atoms.

MO # Energy (eV)	MOs (0.05 isocontour value)	Atoms Simple Distribution
α HOMO-1 (61) -9.990	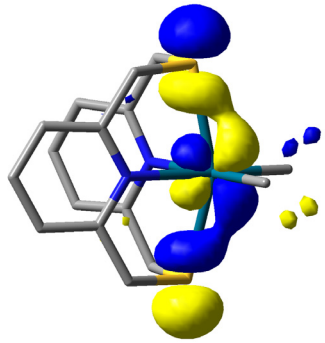	Pd 32% S 46%
α HOMO (62) -7.850	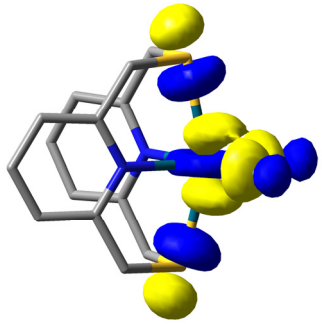	Pd 29% S 40% C 18%
β LUMO (62) -5.578	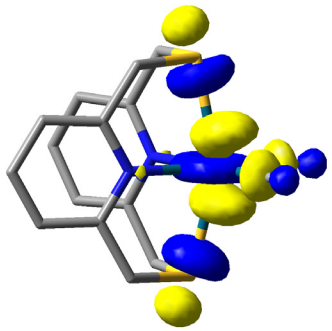	Pd 31% S 34% C 12%

Table S2. Isocontour plots and energies of selected molecular orbitals for $[(^{tBu}N4)Pd^{III}Me_2]^+$. The atomic simple contributions to the MOs are shown for the Pd atoms, the axial amine N atoms (N_{ax}), the equatorial pyridine N atoms (N_{eq}), and the C atoms from the Me group. Balance contribution comes from ligand-based C atoms.

MO # Energy (eV)	MOs (0.05 isocontour value)	Atoms Simple Distribution
α HOMO-1 (85) -9.476	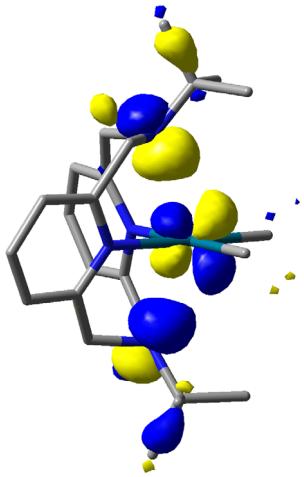	Pd 19% N_{ax} 38%
α HOMO (86) -8.253	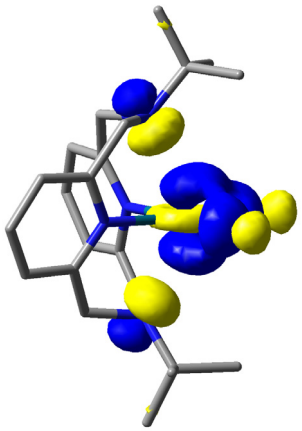	Pd 32% N_{ax} 32% C 16%
β LUMO (86) -5.698	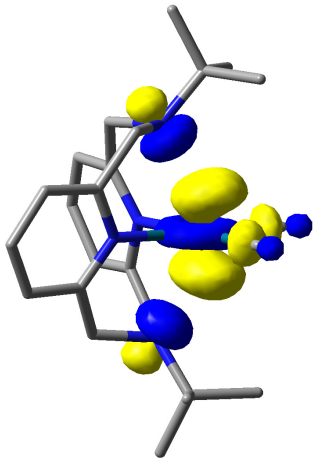	Pd 41% N_{ax} 26% C 10%

Table S3. Isocontour plots and energies of selected molecular orbitals for **4**$^{+}$. The atomic simple contributions to the MOs are shown for the Pd atoms, the S atoms, the equatorial pyridine N atoms (N_{eq}), and the Cl atoms. Balance contribution comes from ligand-based C atoms.

MO # Energy (eV)	MOs (0.05 isocontour value)	Atoms Simple Distribution
α HOMO-4 (58) -10.224	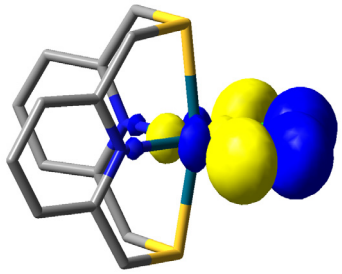	Pd 22% Cl 70%
α HOMO-3 (59) -10.049	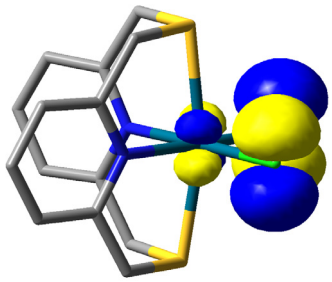	Pd 9% Cl 82%
α HOMO-2 (60) -9.957	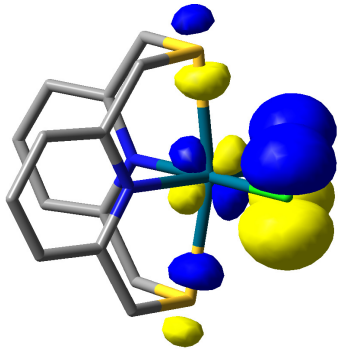	Pd 14% Cl 58% S 24%
α HOMO-1 (61) -9.827	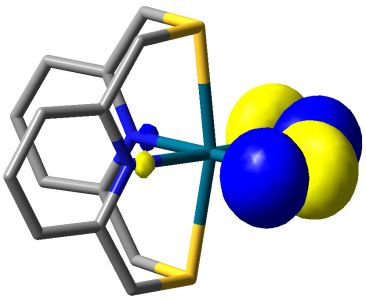	Pd 3% Cl 86% N 6%

α HOMO (62) -8.269	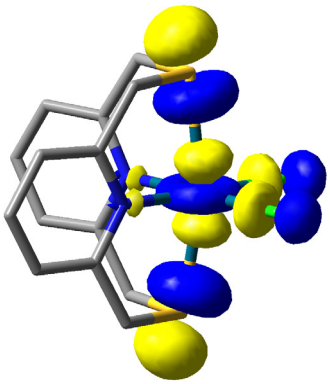	Pd 23% Cl 10% S 44% N 6%
α LUMO (63) –6.502	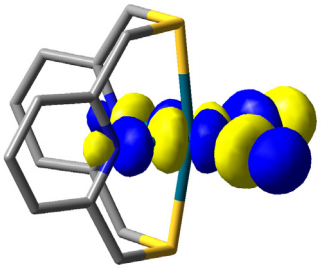	Pd 28% Cl 32% N 22%
β LUMO (62) -6.214	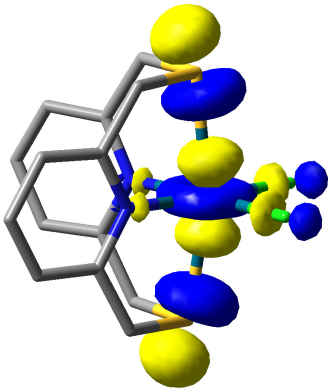	Pd 29% Cl 32% N 22%

Table S4. TD-DFT calculated absorption bands and their composition for **4**$^{+}$. Only the transitions with oscillator strengths greater than 0.005 are listed; the major contributing transitions have more than 10% contribution to the absorption band.

Wavelength (nm)	Oscillator strength	Major contributing transitions
603.3	0.029	β-HOMO → β-LUMO (66%), α-HOMO-4 → α-LUMO (11%)
559.5	0.013	α-HOMO-4 → α-LUMO (51%), β-HOMO → β-LUMO (23%)
397.6	0.017	β-HOMO-5 → β-LUMO (49%), α-HOMO-2 → α-LUMO+1 (32%), β-HOMO-3 → β-LUMO+1 (14%)
390.8	0.014	β-HOMO-5 → β-LUMO (40%), β-HOMO-2 → β-LUMO+1 (30%), β-HOMO-3 → β-LUMO+1 (23%)
358.6	0.064	β-HOMO-6 → β-LUMO (86%), β-HOMO-5 → β-LUMO (10%)
330.6	0.011	β-HOMO-12 → β-LUMO (65%), β-HOMO-15 → β-LUMO (17%)
322.1	0.011	β-HOMO-7 → β-LUMO+1 (34%), α-HOMO-8 → α-LUMO (32%), α-HOMO-12 → α-LUMO (11%)
308.0	0.016	α-HOMO-9 → α-LUMO (55%), α-HOMO-11 → α-LUMO (26%)
306.7	0.014	β-HOMO-10 → β-LUMO+1 (26%), β-HOMO-8 → β-LUMO (25%), β-HOMO-7 → β-LUMO+1 (16%), α-HOMO-12 → α-LUMO (10%)

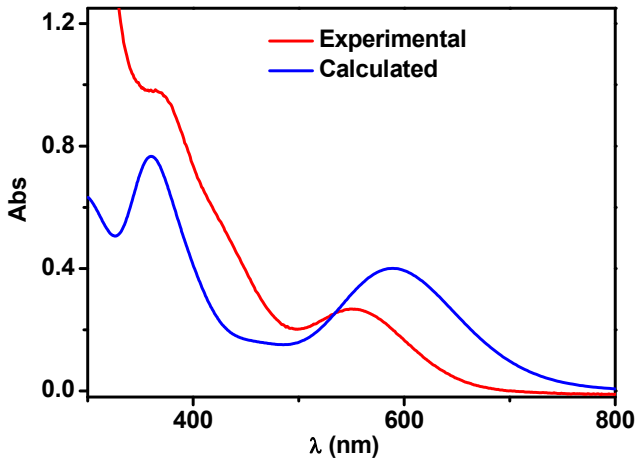

Figure S24. UV-vis spectrum of **4**$^{+}$: experimental spectrum in MeCN (red line); TD-DFT calculated UV-vis spectrum (blue line).

Geometry optimized coordinates of $[(N2S2)Pd^{III}Me_2]^+$ (**1**$^+$)

Pd	-0.14198622	-0.12111706	-0.02054924
S	0.05471525	0.05381541	2.58781067
N	2.15547499	-0.02694085	0.17846737
C	1.87092476	-0.27143861	2.64611831
H	2.29584649	0.20507462	3.54206082
H	1.91178224	-1.36187723	2.81220158
C	2.70836751	0.08468965	1.41143405
C	4.05778696	0.47769223	1.59599027
H	4.47461570	0.55567392	2.60228856
C	4.84770974	0.76038043	0.46004928
H	5.89132285	1.06529457	0.56916811
S	0.48156154	0.44031417	-2.50816844
C	2.28353087	0.08860457	-2.31026638
H	2.85010466	0.67445709	-3.04921857
H	2.35312860	-0.96963199	-2.61632687
C	2.90245949	0.25502616	-0.91739816
C	4.25870356	0.65490570	-0.81915086
H	4.83385492	0.87319434	-1.72137061
N	0.19498977	2.15663072	0.17796127
C	-0.09375383	1.89456285	2.63981796
H	0.40008270	2.27303356	3.54707625
H	-1.17900008	2.04044025	2.77766585
C	0.37451168	2.68615161	1.41324917
C	0.94284867	3.97046430	1.60440660
H	1.07210088	4.36962441	2.61255918
C	1.33182543	4.71963761	0.47192284
H	1.77238917	5.71310961	0.58574867
C	0.33698827	2.27163094	-2.30795665
H	0.98170785	2.76922082	-3.04753826
H	-0.70739458	2.46146813	-2.61018483
C	0.57791150	2.86240119	-0.91408444
C	1.15378891	4.15356130	-0.80970635
H	1.44960201	4.69758718	-1.70912314
C	-2.21370987	-0.12124147	-0.19170576
H	-2.51388834	-0.56892757	-1.15013570
H	-2.65905515	-0.68271393	0.64237560
H	-2.51923411	0.93748857	-0.14963879
C	-0.34768020	-2.18395849	-0.19581076
H	-0.95725974	-2.57483466	0.63181816
H	-0.81513623	-2.43592604	-1.15872296
H	0.67497178	-2.59288997	-0.14668844

Geometry optimized coordinates of $[(^{tBu}N4)Pd^{III}Me_2]^+$

Pd	7.76715481	10.71544008	5.30221707
N	9.42697534	10.13880569	3.99612338
N	9.25332329	9.03235353	6.61234590
N	7.04324891	8.73552155	4.69952985
N	6.82242250	10.92520515	2.88905830
C	9.30158399	10.20343225	2.65393884
C	10.43038595	10.03043140	1.81445101
H	10.33251277	10.11793494	0.72991274
C	11.67446965	9.71309704	2.40708835
H	12.56239759	9.57615194	1.78491409
C	11.74904798	9.52847810	3.80867039
H	12.68061594	9.21921490	4.28733960
C	10.58470351	9.75526140	4.57982322
C	10.56425271	9.55141116	6.10145877
H	11.40516055	8.88271496	6.36301277
H	10.75148007	10.51952750	6.58558816
C	9.18875133	8.97473427	8.14867615
C	10.28969518	8.04999497	8.74986067
H	10.24914597	7.01971846	8.35830887
H	10.15087320	7.98592118	9.84101257
H	11.30346290	8.44521952	8.57575707
C	7.78576253	8.45364868	8.56358059
H	6.98857399	9.06365627	8.11609535
H	7.68844805	8.51496550	9.65868708
H	7.61811066	7.40081762	8.28740214
C	9.36364457	10.39408947	8.74695400
H	10.37203299	10.80753941	8.58881732
H	9.20993483	10.34130219	9.83623563
H	8.62495584	11.09193826	8.33167496
C	8.91269507	7.71568661	5.98549846
H	8.96349810	6.89742972	6.71674702
H	9.67753982	7.47418334	5.22736712
C	7.56822861	7.61582054	5.23901595
C	6.05788674	8.67776413	3.77492867
C	5.66278146	9.99649447	3.09663836
H	5.15528136	9.74953862	2.14583822
H	4.93378340	10.51274413	3.73598456
C	6.39989076	12.29734196	2.33740116
C	5.67641640	12.18078300	0.96227526
H	6.28106031	11.66113116	0.20025470
H	5.46951344	13.19169602	0.57602612
H	4.70781089	11.66180734	1.04551050
C	5.44791888	13.00621553	3.33409564

Geometry optimized coordinates of $[(N2S2)Pd^{III}Cl_2]^+$ (**4**$^+$)

Pd	0.03787997	0.03218894	0.00612563
S	0.05788381	0.05214058	2.56799675
N	2.16289488	0.00780326	0.18268193
C	1.86836169	-0.29001977	2.65501104
H	2.29495968	0.20498733	3.54004697
H	1.89192539	-1.37698177	2.84494728
C	2.72656624	0.00197844	1.41976945
C	4.11982303	0.18963270	1.58683436
H	4.55322297	0.17850708	2.58881848
C	4.93022075	0.37841643	0.44615318
H	6.00796442	0.52511297	0.54896689
S	0.48533811	0.43013680	-2.48670212
C	2.29105756	0.09150865	-2.32012059
H	2.85027937	0.71389175	-3.03447320
H	2.36608479	-0.95326845	-2.66776395
C	2.92587216	0.18240477	-0.92864996
C	4.32491109	0.37578392	-0.82938092
H	4.92021239	0.51180607	-1.73441403
N	0.24291564	2.14811118	0.17997909
C	-0.08804693	1.89008113	2.65034690
H	0.43938444	2.26323417	3.54080242
H	-1.16855062	2.03023435	2.82637979
C	0.30872225	2.70790697	1.41698156
C	0.66824398	4.06712491	1.58303425
H	0.71415865	4.49910562	2.58465994
C	0.95298983	4.84750638	0.44125802
H	1.23421594	5.89827439	0.54343290
C	0.32254278	2.26161771	-2.32009254
H	0.97814324	2.75915299	-3.05006971
H	-0.71885693	2.43252416	-2.64320138
C	0.50411761	2.88385495	-0.93252004
C	0.86939157	4.24815985	-0.83454253
H	1.07391985	4.82286589	-1.73997542
Cl	-2.28605016	0.23891246	-0.17366581
Cl	-0.00822626	-2.30057256	-0.16750633

VII. ^{1}H NMR of (N2S2)Pd complexes

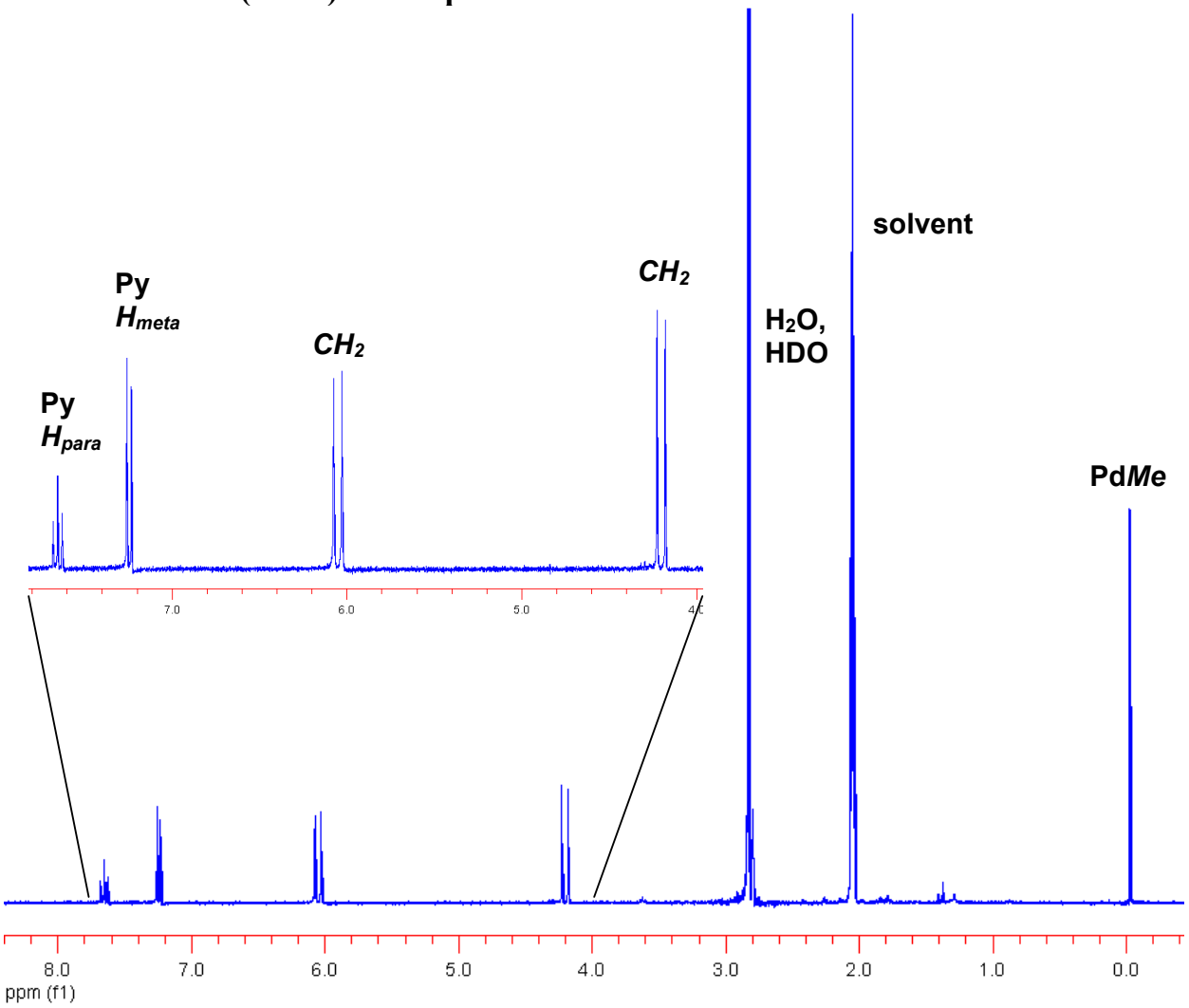

Figure S25. ^{1}H NMR spectrum of (N2S2)Pd^{II}Me$_2$ (**1**) in acetone-d_6.

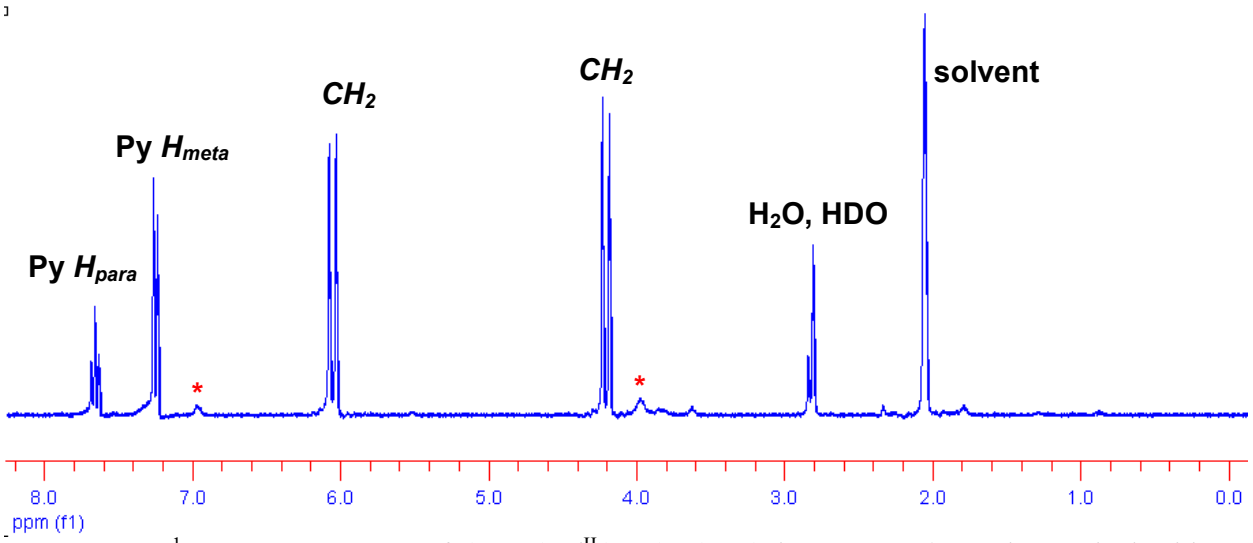

Figure S26. ^{1}H NMR spectrum of (N2S2)Pd^{II}(CD$_3$)$_2$ (**1-*d*$_6$**) in acetone-d_6. Peaks marked with an asterisk correspond to a trace amount of free N2S2 ligand in the sample.

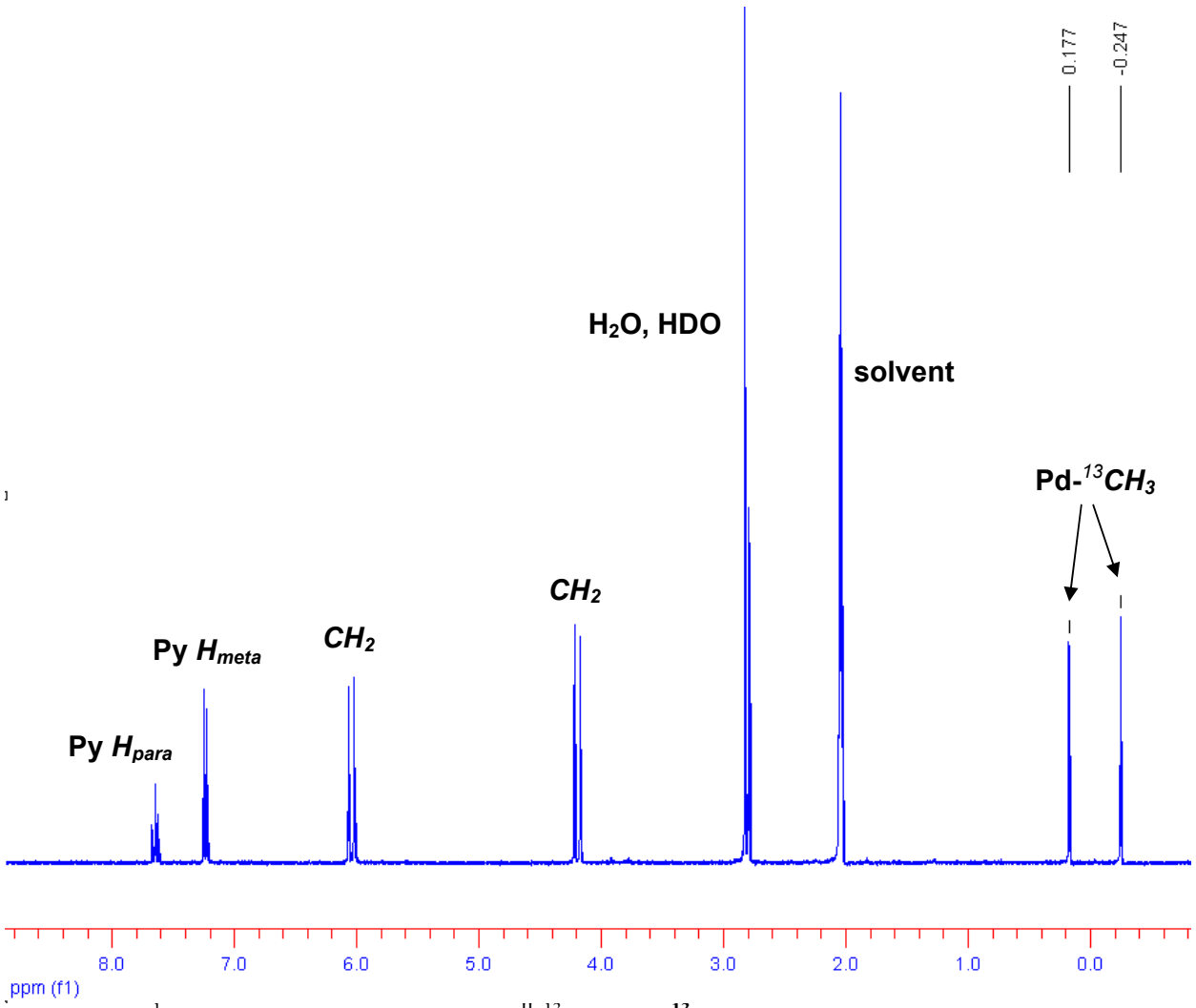

Figure S27. ^{1}H NMR spectrum of (N2S2)Pd^{II}(^{13}CH$_3$)$_2$ (**1-^{13}C**) in acetone-d_6.

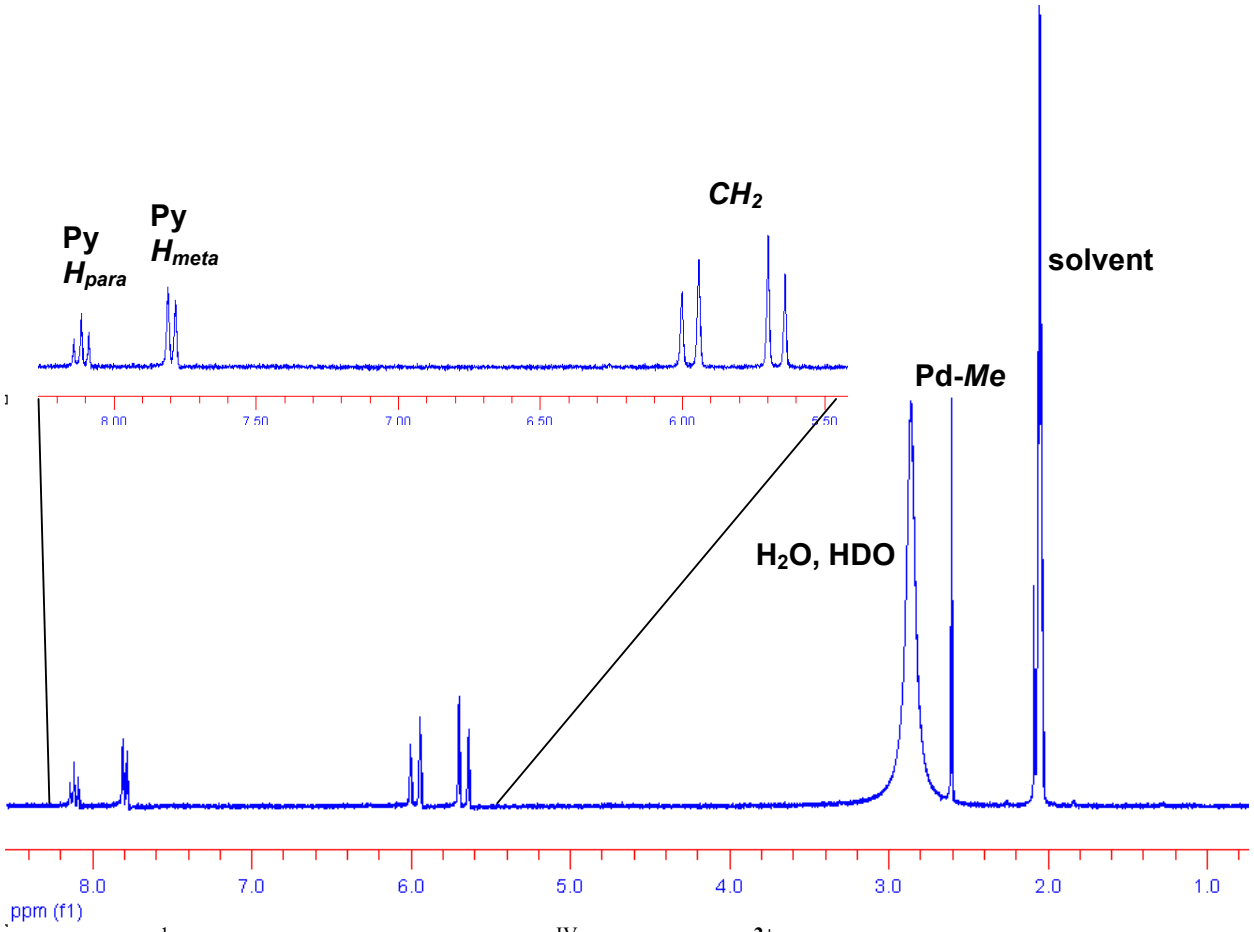

Figure S28. ^{1}H NMR spectrum of [(N2S2)Pd^{IV}Me$_2$](PF$_6$)$_2$ (**[1^{2+}](PF$_6$)$_2$**) in acetone-d_6.

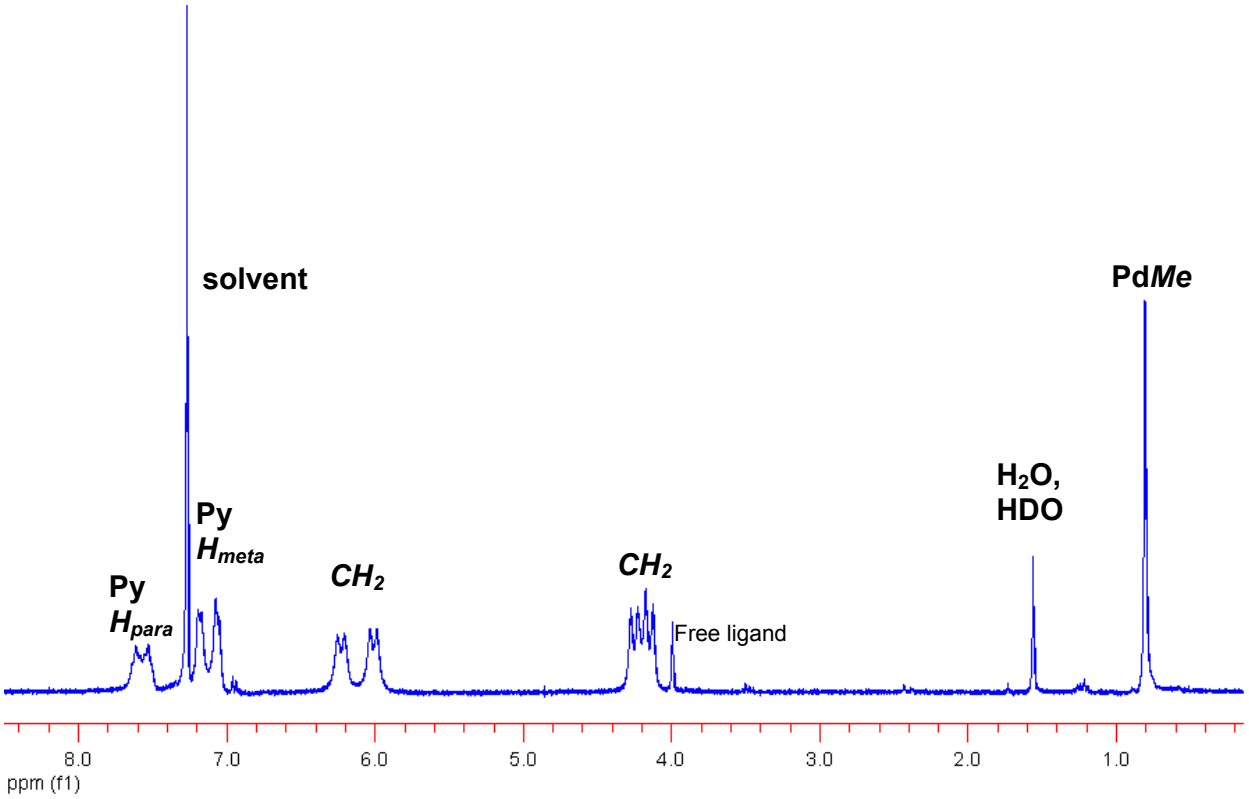

Figure S29. ^{1}H NMR spectrum of (N2S2)Pd^{II}MeCl (**2**) in $CDCl_3$.

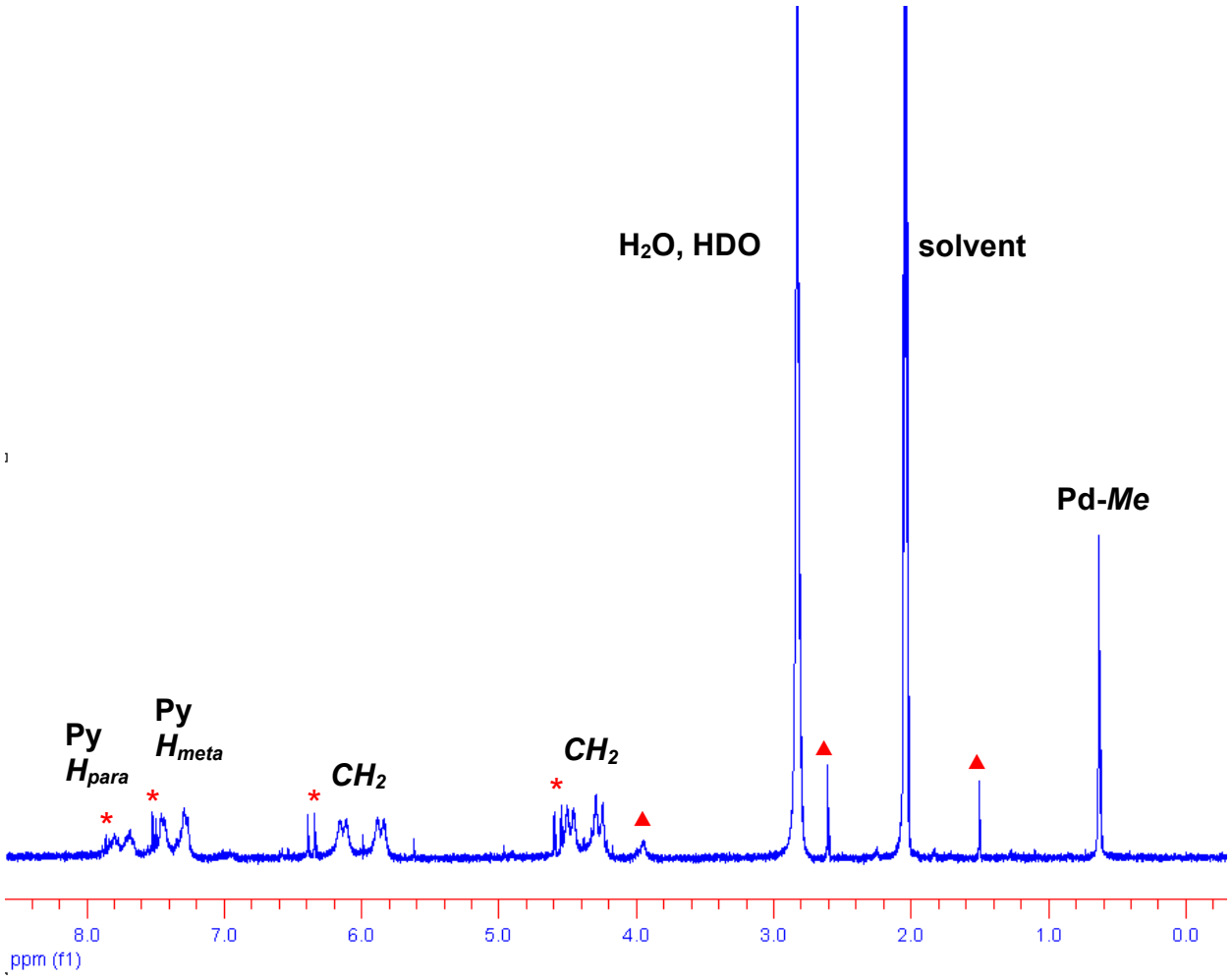

Figure S30. ^{1}H NMR spectrum of (N2S2)Pd^{II}MeBr (**3**) in acetone-d_6. Peaks marked with asterisks correspond to the side product of (N2S2)Pd^{II}BrCl with 10-20%. Peaks marked with triangles correspond to a trace amount of free N2S2 ligand (< 5%) and decomposition upon dissolution.

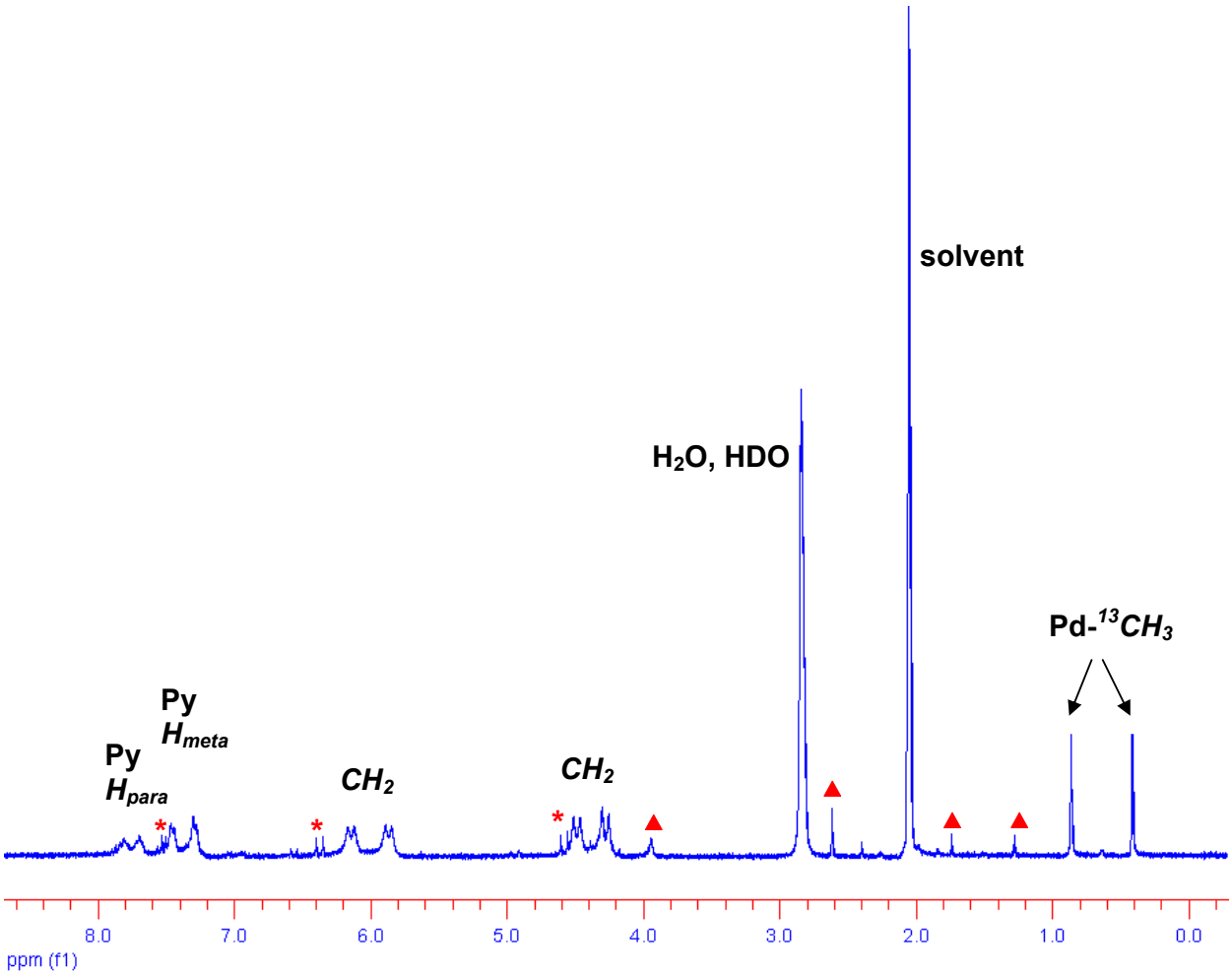

Figure S31. ^{1}H NMR spectrum of (N2S2)Pd^{II}(^{13}CH$_3$)Br (**3-^{13}C**) in acetone-d_6. Peaks marked with asterisks correspond to the side product of (N2S2)Pd^{II}BrCl with 10-20%. Peaks marked with triangles correspond to a trace amount of free N2S2 ligand (< 5%) and decomposition upon dissolution.

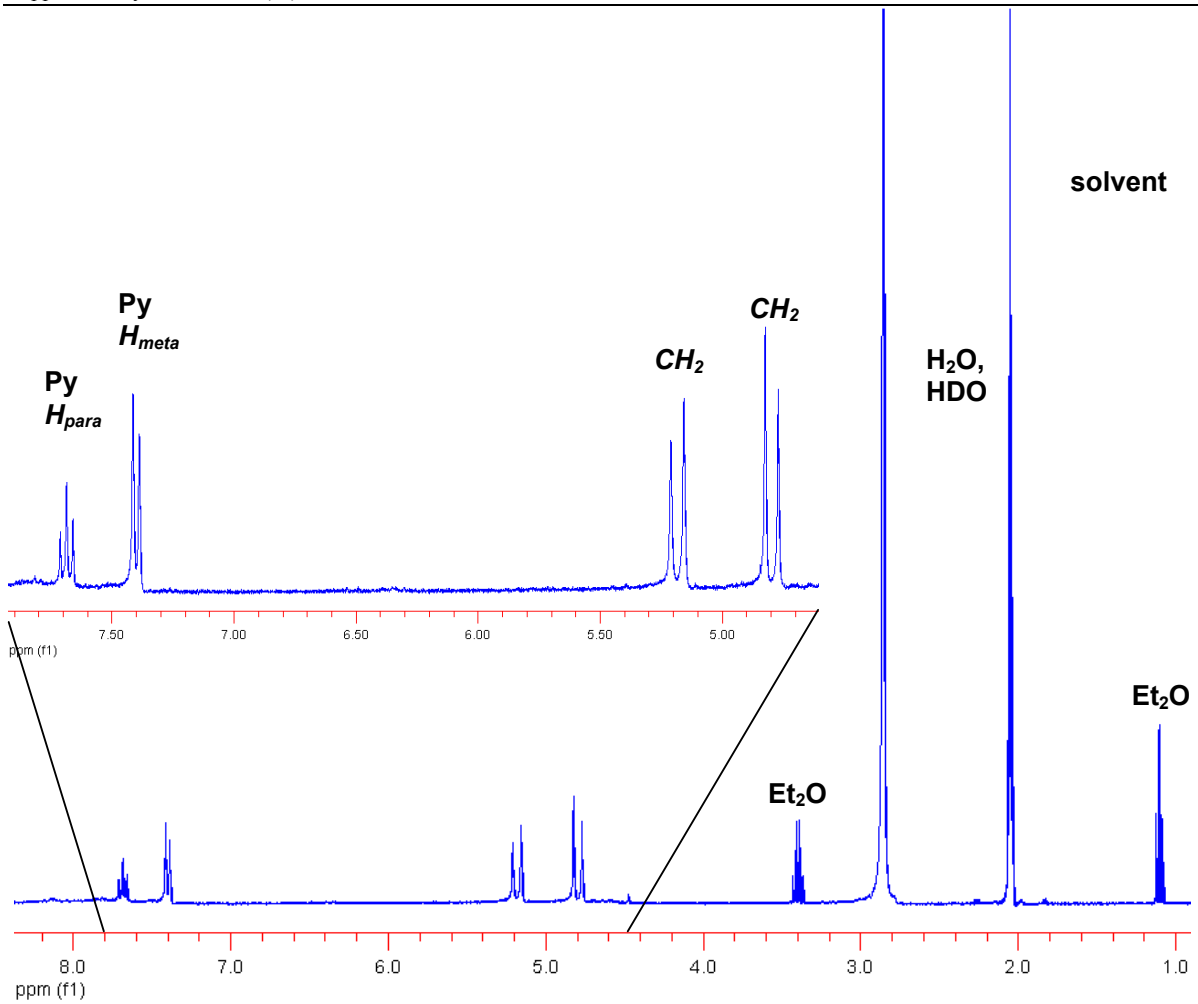

Figure S32. ^{1}H NMR spectrum of [(N2S2)Pd^{II}Cl](OTf) (**6**) in CD_3CN.

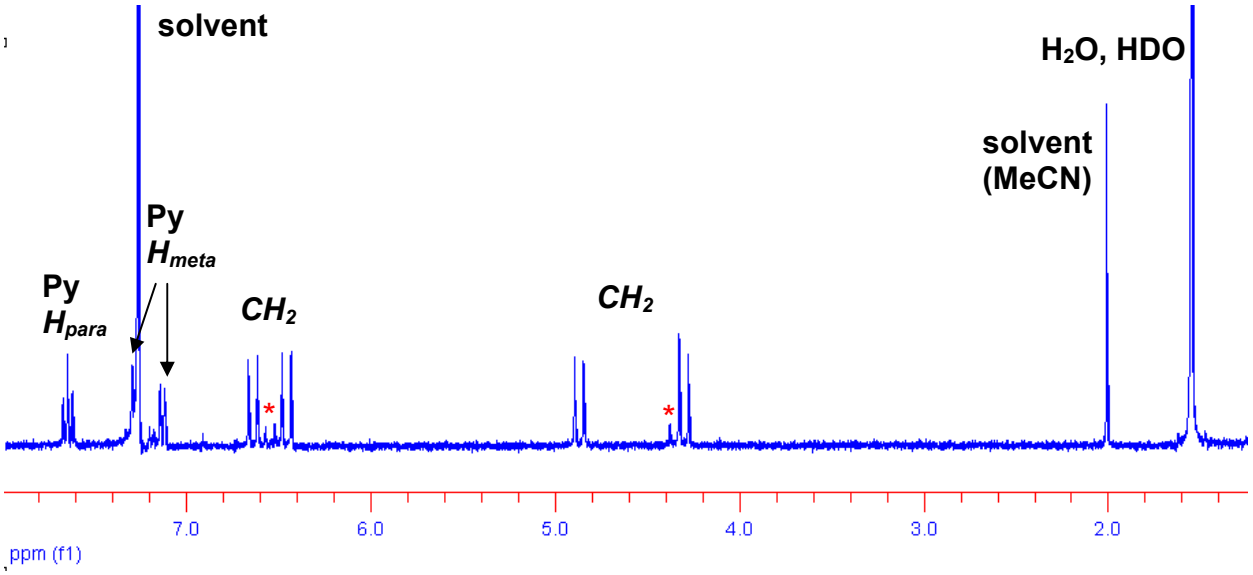

Figure S33. ^{1}H NMR spectrum of (N2S2-O)Pd^{II}Cl$_2$ (**7**) in $CDCl_3$. Peaks marked with asterisks correspond to the starting material of (N2S2)Pd^{II}Cl$_2$ (**4**).

VIII. X-ray crystal structure determination of 1, $1^{2+}(PF_6)_2$ and 6-Cl

1) $(N2S2)Pd^{II}Me_2$, **1** (lm6012.cif)

Table 1. Crystal data and structure refinement for lm6012.

Identification code	l6012/lt/JL0228-1	
Empirical formula	$C_{16}H_{20}N_2PdS_2$	
Formula weight	410.86	
Temperature	100(2) K	
Wavelength	0.71073 Å	
Crystal system	Monoclinic	
Space group	$P2_1/c$	
Unit cell dimensions	a = 12.293(6) Å	α= 90°.
	b = 8.458(4) Å	β= 90.93(3)°.
	c = 15.964(8) Å	γ = 90°.
Volume	1659.8(14) $Å^3$	
Z	4	
Density (calculated)	1.644 Mg/m^3	
Absorption coefficient	1.364 mm^{-1}	
F(000)	832	
Crystal size	0.20 x 0.20 x 0.09 mm^3	
Theta range for data collection	1.66 to 27.62°.	
Index ranges	$-15 \le h \le 16$, $-10 \le k \le 9$, $-20 \le l \le 20$	
Reflections collected	30260	
Independent reflections	3809 [R(int) = 0.0870]	
Completeness to theta = 27.62°	98.7 %	
Absorption correction	Semi-empirical	
Max. and min. transmission	0.8848 and 0.7683	
Refinement method	Full-matrix least-squares on F^2	
Data / restraints / parameters	3809 / 0 / 192	
Goodness-of-fit on F^2	1.176	
Final R indices [I>2sigma(I)]	R1 = 0.0436, wR2 = 0.1217	
R indices (all data)	R1 = 0.0530, wR2 = 0.1268	
Largest diff. peak and hole	0.710 and -0.909 $e.Å^{-3}$	

Table 2. Bond lengths [Å] for lm6012.

Pd(1)-C(2)	2.035(4)
Pd(1)-C(1)	2.043(5)
Pd(1)-N(1)	2.184(3)
Pd(1)-N(2)	2.194(3)
S(1)-C(9)	1.827(4)
S(1)-C(8)	1.829(4)
S(2)-C(16)	1.810(4)
S(2)-C(15)	1.817(4)
N(1)-C(7)	1.351(5)
N(1)-C(3)	1.361(5)
N(2)-C(10)	1.353(5)
N(2)-C(14)	1.358(5)
C(1)-H(1A)	0.9800
C(1)-H(1B)	0.9800
C(1)-H(1C)	0.9800
C(2)-H(2A)	0.9800
C(2)-H(2B)	0.9800
C(2)-H(2C)	0.9800
C(3)-C(4)	1.396(6)
C(3)-C(16)	1.490(6)
C(4)-C(5)	1.374(7)
C(4)-H(4)	0.9500
C(5)-C(6)	1.375(7)
C(5)-H(5)	0.9500
C(6)-C(7)	1.383(6)
C(6)-H(6)	0.9500
C(7)-C(8)	1.513(6)
C(8)-H(8A)	0.9900
C(8)-H(8B)	0.9900
C(9)-C(10)	1.504(5)
C(9)-H(9A)	0.9900
C(9)-H(9B)	0.9900
C(10)-C(11)	1.402(6)

C(11)-C(12)	1.398(6)
C(11)-H(11)	0.9500
C(12)-C(13)	1.384(7)
C(12)-H(12)	0.9500
C(13)-C(14)	1.390(6)
C(13)-H(13)	0.9500
C(14)-C(15)	1.505(6)
C(15)-H(15A)	0.9900
C(15)-H(15B)	0.9900
C(16)-H(16A)	0.9900
C(16)-H(16B)	0.9900

Projection view with 50% thermal ellipsoids:

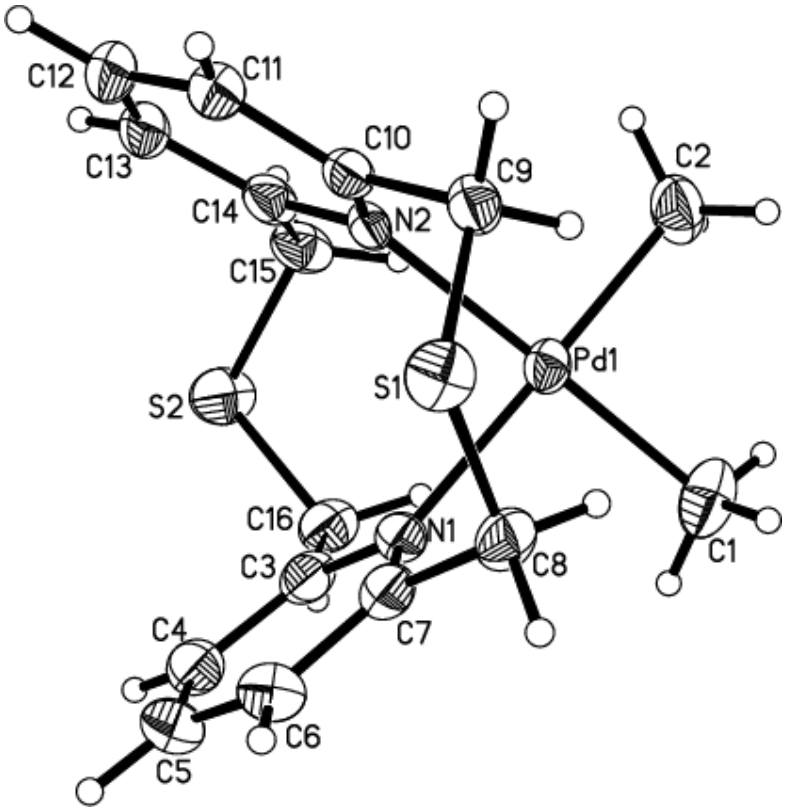

2) $[(N2S2)Pd^{IV}Me_2](PF_6)_2$, $\mathbf{1^{2+}(PF_6)_2}$ (lm18111.cif)

Table 1. Crystal data and structure refinement for lm18111.

Identification code	l18111/lt/Jl111129-1	
Empirical formula	$C_{76}\ H_{104}\ F_{48}\ N_8\ O_4\ P_8\ Pd_4\ S_8$	
Formula weight	3035.51	
Temperature	100(2) K	
Wavelength	0.71073 Å	
Crystal system	Orthorhombic	
Space group	I m m a	
Unit cell dimensions	a = 15.2927(8) Å	α= 90°.
	b = 17.3479(9) Å	β= 90°.
	c = 9.7829(5) Å	γ = 90°.
Volume	2595.4(2) $Å^3$	
Z	1	
Density (calculated)	1.942 Mg/m^3	
Absorption coefficient	1.105 mm^{-1}	
F(000)	1512	
Crystal size	0.290 x 0.220 x 0.120 mm^3	
Theta range for data collection	2.348 to 27.497°.	
Index ranges	$-19 \le h \le 19$, $-22 \le k \le 22$, $-12 \le l \le 12$	
Reflections collected	23422	
Independent reflections	1605 [R(int) = 0.0560]	
Completeness to theta = 25.242°	99.9 %	
Absorption correction	Semi-empirical from equivalents	
Max. and min. transmission	0.7461 and 0.6639	
Refinement method	Full-matrix least-squares on F^2	
Data / restraints / parameters	1605 / 30 / 111	
Goodness-of-fit on F^2	1.067	
Final R indices [I>2sigma(I)]	R1 = 0.0702, wR2 = 0.2141	
R indices (all data)	R1 = 0.0720, wR2 = 0.2152	
Extinction coefficient	n/a	
Largest diff. peak and hole	1.585 and -1.836 $e.Å^{-3}$	

Table 2. Bond lengths [Å] for lm18111.

Pd(1)-C(1)	2.082(11)
Pd(1)-C(1)#1	2.082(11)
Pd(1)-N(1)#1	2.151(8)
Pd(1)-N(1)	2.151(8)
Pd(1)-S(1)#1	2.323(2)
Pd(1)-S(1)	2.323(2)
S(1)-C(2)#2	1.836(8)
S(1)-C(2)	1.836(8)
N(1)-C(3)#3	1.335(8)
N(1)-C(3)	1.335(8)
C(1)-H(1A)	0.9800
C(1)-H(1B)	0.9800
C(1)-H(1C)	0.9800
C(2)-C(3)	1.511(10)
C(2)-H(2A)	0.9900
C(2)-H(2B)	0.9900
C(3)-C(4)	1.391(10)
C(4)-C(5)	1.395(10)
C(4)-H(4)	0.9500
C(5)-C(4)#3	1.395(10)
C(5)-H(5)	0.9500
P(1)-F(3')	1.485(10)
P(1)-F(1)	1.582(6)
P(1)-F(1)#4	1.582(6)
P(1)-F(2)	1.608(6)
P(1)-F(2)#4	1.608(6)
P(1)-F(3)#4	1.781(12)
P(1)-F(3)	1.781(12)
O(1S)-C(1S)	1.2149
C(1S)-C(2SA)	1.2486
C(1S)-C(2S)	1.6620
C(2S)-H(2S1)	0.9800
C(2S)-H(2S2)	0.9800
C(2S)-H(2S3)	0.9800

C(2SA)-H(2S4)	0.9800
C(2SA)-H(2S5)	0.9800
C(2SA)-H(2S6)	0.9800

Projection view with 50% thermal ellipsoids:

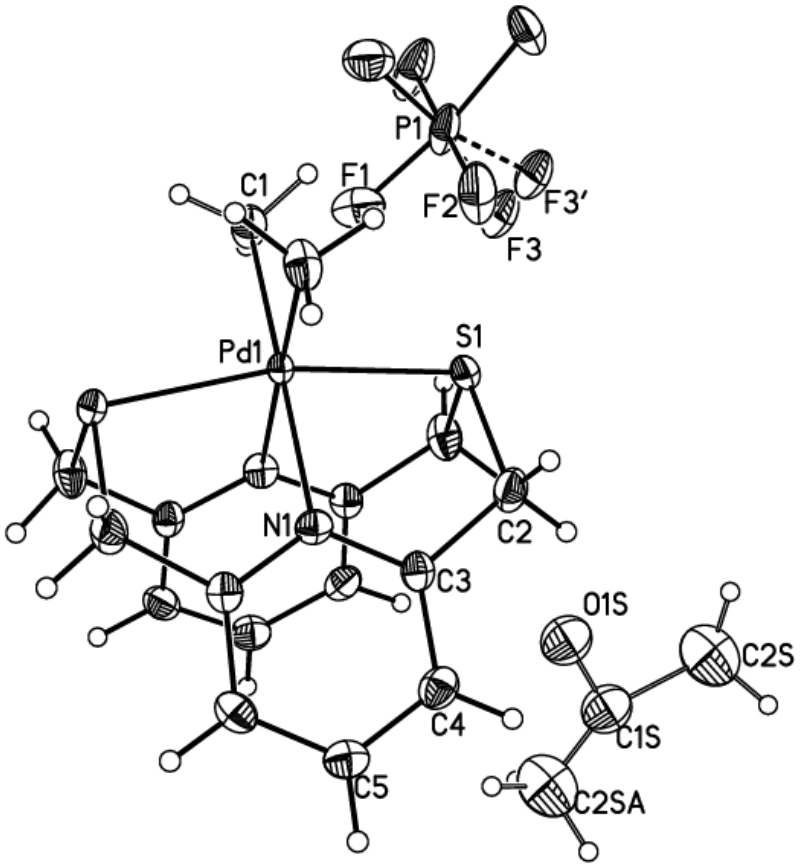

3) [(N2S2)Pd^{II}Cl](OTf), **6-Cl** (lm7811.cif)

Table 1. Crystal data and structure refinement for lm7811.

Identification code	l7811/lt/smart/JL051811	
Empirical formula	C_{15} H_{14} Cl F_3 N_2 O_3 Pd S_3	
Formula weight	565.31	
Temperature	100(2) K	
Wavelength	0.71073 Å	
Crystal system	Triclinic	
Space group	P-1	
Unit cell dimensions	a = 8.3576(4) Å	α= 106.125(3)°.
	b = 15.8701(9) Å	β= 91.626(3)°.
	c = 23.2350(13) Å	γ = 99.216(3)°.
Volume	2913.7(3) Å^3	
Z	6	
Density (calculated)	1.933 Mg/m^3	
Absorption coefficient	1.463 mm^{-1}	
F(000)	1680	
Crystal size	0.47 x 0.28 x 0.08 mm^3	
Theta range for data collection	1.83 to 27.63°.	
Index ranges	-10≤h≤10, -20≤k≤20, -30≤l≤30	
Reflections collected	71180	
Independent reflections	13260 [R(int) = 0.0382]	
Completeness to theta = 25.00°	99.4 %	
Absorption correction	Semi-empirical from equivalents	
Max. and min. transmission	0.8969 and 0.5475	
Refinement method	Full-matrix least-squares on F^2	
Data / restraints / parameters	13260 / 0 / 757	
Goodness-of-fit on F^2	1.150	
Final R indices [I>2sigma(I)]	R1 = 0.0313, wR2 = 0.0630	
R indices (all data)	R1 = 0.0462, wR2 = 0.0747	
Largest diff. peak and hole	0.872 and -0.651 e.Å^{-3}	

Table 2. Bond lengths [Å] for lm7811.

Pd(1)-N(1)	2.022(3)
Pd(1)-Cl(1)	2.2826(8)
Pd(1)-S(1)	2.3217(8)
Pd(1)-S(2)	2.3234(8)
Pd(2)-N(3)	2.037(3)
Pd(2)-Cl(2)	2.3069(8)
Pd(2)-S(4)	2.3251(9)
Pd(2)-S(3)	2.3281(8)
Pd(3)-N(5)	2.030(3)
Pd(3)-Cl(3)	2.2855(9)
Pd(3)-S(5)	2.3085(8)
Pd(3)-S(6)	2.3355(9)
Pd(3)-N(6)	2.573(3)
S(1)-C(6)	1.817(3)
S(1)-C(7)	1.844(3)
S(2)-C(14)	1.810(3)
S(2)-C(13)	1.840(3)
S(3)-C(20)	1.817(3)
S(3)-C(21)	1.848(3)
S(4)-C(28)	1.818(4)
S(4)-C(27)	1.850(4)
S(5)-C(34)	1.820(3)
S(5)-C(35)	1.846(3)
S(6)-C(42)	1.819(4)
S(6)-C(41)	1.845(4)
S(7)-O(2)	1.435(3)
S(7)-O(3)	1.436(3)
S(7)-O(1)	1.440(3)
S(7)-C(43)	1.815(4)
S(8)-O(6)	1.440(3)
S(8)-O(4)	1.441(3)
S(8)-O(5)	1.445(2)
S(8)-C(44)	1.832(4)

S(9)-O(8)	1.439(3)
S(9)-O(7)	1.442(2)
S(9)-O(9)	1.449(3)
S(9)-C(45)	1.831(4)
F(1)-C(43)	1.328(4)
F(2)-C(43)	1.341(4)
F(3)-C(43)	1.337(4)
F(4)-C(44)	1.336(5)
F(5)-C(44)	1.328(4)
F(6)-C(44)	1.346(4)
F(7)-C(45)	1.334(5)
F(8)-C(45)	1.331(5)
F(9)-C(45)	1.329(5)
N(1)-C(5)	1.347(4)
N(1)-C(1)	1.363(4)
N(2)-C(12)	1.338(4)
N(2)-C(8)	1.343(4)
N(3)-C(19)	1.349(4)
N(3)-C(15)	1.360(4)
N(4)-C(22)	1.331(4)
N(4)-C(26)	1.344(4)
N(5)-C(33)	1.351(4)
N(5)-C(29)	1.358(4)
N(6)-C(36)	1.333(4)
N(6)-C(40)	1.337(4)
C(1)-C(2)	1.373(5)
C(1)-C(14)	1.502(4)
C(2)-C(3)	1.392(5)
C(2)-H(2)	0.9500
C(3)-C(4)	1.380(5)
C(3)-H(3)	0.9500
C(4)-C(5)	1.388(4)
C(4)-H(4)	0.9500
C(5)-C(6)	1.509(4)
C(6)-H(6A)	0.9900

C(6)-H(6B)	0.9900
C(7)-C(8)	1.496(4)
C(7)-H(7A)	0.9900
C(7)-H(7B)	0.9900
C(8)-C(9)	1.394(5)
C(9)-C(10)	1.382(5)
C(9)-H(9)	0.9500
C(10)-C(11)	1.390(5)
C(10)-H(10)	0.9500
C(11)-C(12)	1.385(5)
C(11)-H(11)	0.9500
C(12)-C(13)	1.512(4)
C(13)-H(13A)	0.9900
C(13)-H(13B)	0.9900
C(14)-H(14A)	0.9900
C(14)-H(14B)	0.9900
C(15)-C(16)	1.390(5)
C(15)-C(28)	1.491(5)
C(16)-C(17)	1.376(5)
C(16)-H(16)	0.9500
C(17)-C(18)	1.386(5)
C(17)-H(17)	0.9500
C(18)-C(19)	1.393(5)
C(18)-H(18)	0.9500
C(19)-C(20)	1.509(4)
C(20)-H(20A)	0.9900
C(20)-H(20B)	0.9900
C(21)-C(22)	1.513(5)
C(21)-H(21A)	0.9900
C(21)-H(21B)	0.9900
C(22)-C(23)	1.393(5)
C(23)-C(24)	1.390(5)
C(23)-H(23)	0.9500
C(24)-C(25)	1.379(6)
C(24)-H(24)	0.9500

C(25)-C(26)	1.391(5)
C(25)-H(25)	0.9500
C(26)-C(27)	1.504(5)
C(27)-H(27A)	0.9900
C(27)-H(27B)	0.9900
C(28)-H(28A)	0.9900
C(28)-H(28B)	0.9900
C(29)-C(30)	1.384(5)
C(29)-C(42)	1.498(5)
C(30)-C(31)	1.386(5)
C(30)-H(30)	0.9500
C(31)-C(32)	1.384(5)
C(31)-H(31)	0.9500
C(32)-C(33)	1.389(5)
C(32)-H(32)	0.9500
C(33)-C(34)	1.509(5)
C(34)-H(34A)	0.9900
C(34)-H(34B)	0.9900
C(35)-C(36)	1.503(5)
C(35)-H(35A)	0.9900
C(35)-H(35B)	0.9900
C(36)-C(37)	1.398(5)
C(37)-C(38)	1.386(5)
C(37)-H(37)	0.9500
C(38)-C(39)	1.386(5)
C(38)-H(38)	0.9500
C(39)-C(40)	1.392(5)
C(39)-H(39)	0.9500
C(40)-C(41)	1.512(5)
C(41)-H(41A)	0.9900
C(41)-H(41B)	0.9900
C(42)-H(42A)	0.9900
C(42)-H(42B)	0.9900

Projection view with 50% thermal ellipsoids- H atom omitted:

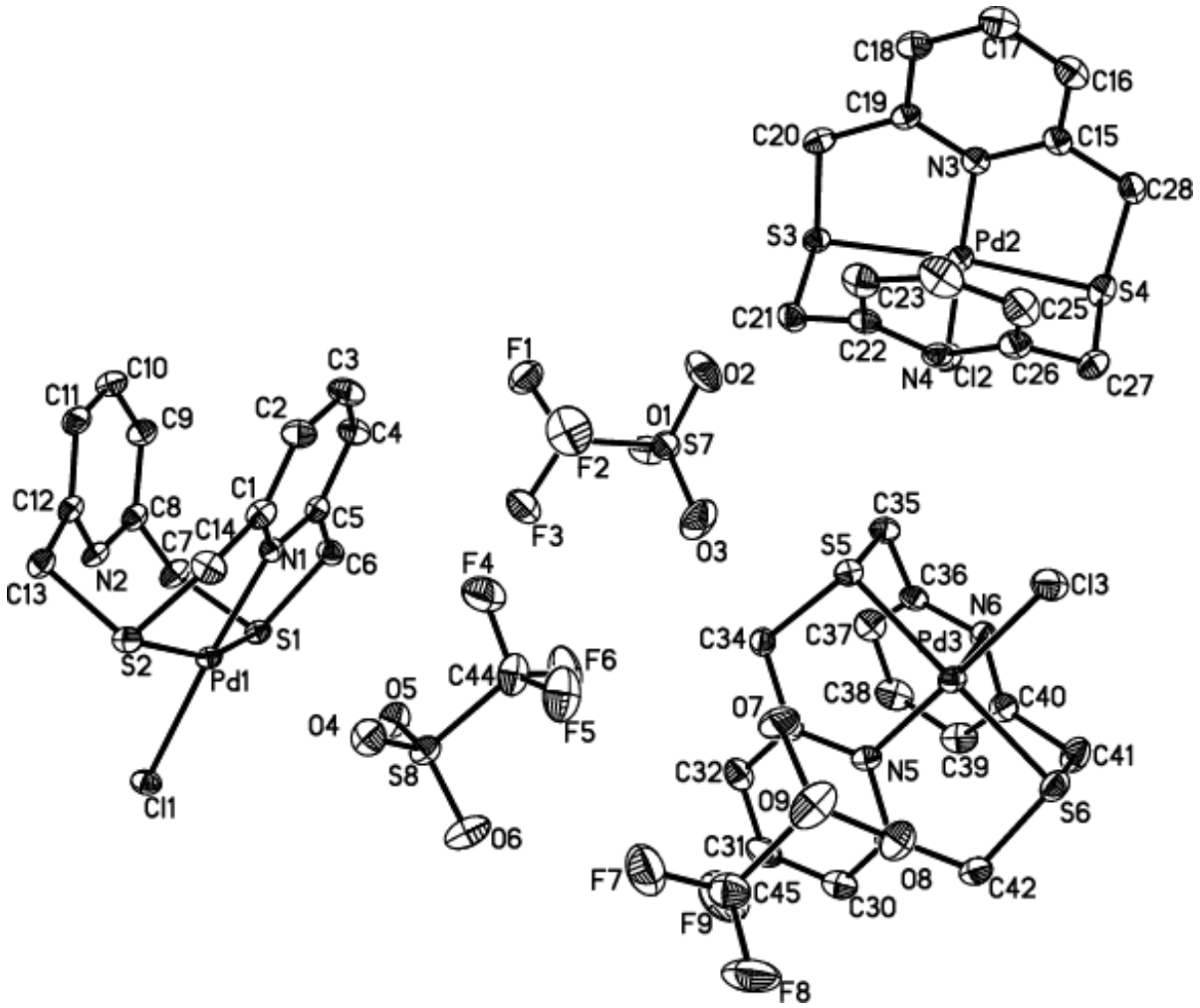

IX. Preliminary crystal structures of 3 and 7

1) (N2S2)Pd^{II}MeBr, **3** (lm6212).

Table 1. Crystal data and structure refinement for lm6212.

Identification code	l6212/lt/Jl022812-2	
Empirical formula	$C_{14.75}$ $H_{16.25}$ Br $Cl_{0.25}$ N_2 Pd S_2	
Formula weight	480.84	
Temperature	100(2) K	
Wavelength	0.71073 Å	
Crystal system	Monoclinic	
Space group	$P2_1/c$	
Unit cell dimensions	a = 12.3042(7) Å	α= 90°.
	b = 8.5481(5) Å	β= 91.830(3)°.
	c = 15.8623(9) Å	γ = 90°.
Volume	1667.51(17) $Å^3$	
Z	4	
Density (calculated)	1.915 Mg/m^3	
Absorption coefficient	3.793 mm^{-1}	
F(000)	944	
Crystal size	0.19 x 0.16 x 0.08 mm^3	
Theta range for data collection	1.66 to 27.14°.	
Index ranges	$-15 \leq h \leq 15$, $-10 \leq k \leq 10$, $-20 \leq l \leq 18$	
Reflections collected	22828	
Independent reflections	3678 [R(int) = 0.0487]	
Completeness to theta = 27.14°	99.5 %	
Absorption correction	Semi-empirical from equivalents	
Max. and min. transmission	0.7589 and 0.5311	
Refinement method	Full-matrix least-squares on F^2	
Data / restraints / parameters	3678 / 46 / 217	
Goodness-of-fit on F^2	1.156	
Final R indices [I>2sigma(I)]	R1 = 0.0571, wR2 = 0.1404	
R indices (all data)	R1 = 0.0706, wR2 = 0.1463	
Largest diff. peak and hole	0.829 and -0.790 $e.Å^{-3}$	

Table 2. Bond lengths [Å] and angles [°] for lm6212.

Pd(1)-Cl(1)	2.08(2)
Pd(1)-Cl(1')	2.08(2)
Pd(1)-N(1)	2.121(6)
Pd(1)-C(1')	2.13(2)
Pd(1)-C(1)	2.13(2)
Pd(1)-N(2)	2.142(6)
Pd(1)-Br(1')	2.390(4)
Pd(1)-Br(1)	2.3983(17)
S(1)-C(7)	1.822(7)
S(1)-C(8)	1.837(8)
S(2)-C(14)	1.818(7)
S(2)-C(15)	1.821(7)
S(2')-C(15)	1.870(8)
S(2')-C(14)	1.878(8)
N(1)-C(2)	1.359(8)
N(1)-C(6)	1.369(9)
N(2)-C(13)	1.341(9)
N(2)-C(9)	1.349(9)
C(2)-C(3)	1.395(12)
C(2)-C(15)	1.466(13)
C(3)-C(4)	1.357(14)
C(3)-H(3)	0.9500
C(4)-C(5)	1.404(11)
C(4)-H(4)	0.9500
C(5)-C(6)	1.384(11)
C(5)-H(5)	0.9500
C(6)-C(7)	1.493(9)
C(7)-H(7A)	0.9900
C(7)-H(7B)	0.9900
C(8)-C(9)	1.485(9)
C(8)-H(8A)	0.9900
C(8)-H(8B)	0.9900
C(9)-C(10)	1.391(10)

C(10)-C(11)	1.398(12)
C(10)-H(10)	0.9500
C(11)-C(12)	1.363(14)
C(11)-H(11)	0.9500
C(12)-C(13)	1.380(13)
C(12)-H(12)	0.9500
C(13)-C(14)	1.481(12)
C(14)-H(14A)	0.9900
C(14)-H(14B)	0.9900
C(15)-H(15A)	0.9900
C(15)-H(15B)	0.9900
C(1)-H(1A)	0.9800
C(1)-H(1B)	0.9800
C(1)-H(1C)	0.9800
C(1')-H(1'A)	0.9800
C(1')-H(1'B)	0.9800
C(1')-H(1'C)	0.9800

Cl(1)-Pd(1)-Cl(1')	124(3)
Cl(1)-Pd(1)-N(1)	98.0(8)
Cl(1')-Pd(1)-N(1)	137(3)
Cl(1)-Pd(1)-C(1')	14.8(9)
Cl(1')-Pd(1)-C(1')	133(3)
N(1)-Pd(1)-C(1')	87.5(10)
Cl(1)-Pd(1)-C(1)	93.4(9)
Cl(1')-Pd(1)-C(1)	33(4)
N(1)-Pd(1)-C(1)	167.0(6)
C(1')-Pd(1)-C(1)	104.8(10)
Cl(1)-Pd(1)-N(2)	173.2(8)
Cl(1')-Pd(1)-N(2)	52(3)
N(1)-Pd(1)-N(2)	86.4(2)
C(1')-Pd(1)-N(2)	171.9(10)
C(1)-Pd(1)-N(2)	81.8(6)
Cl(1)-Pd(1)-Br(1')	3.8(10)
Cl(1')-Pd(1)-Br(1')	124(3)

N(1)-Pd(1)-Br(1')	98.3(3)
C(1')-Pd(1)-Br(1')	12.7(10)
C(1)-Pd(1)-Br(1')	93.5(6)
N(2)-Pd(1)-Br(1')	175.2(3)
Cl(1)-Pd(1)-Br(1)	80.9(8)
Cl(1')-Pd(1)-Br(1)	44(3)
N(1)-Pd(1)-Br(1)	178.06(16)
C(1')-Pd(1)-Br(1)	91.1(10)
C(1)-Pd(1)-Br(1)	14.8(6)
N(2)-Pd(1)-Br(1)	94.92(17)
Br(1')-Pd(1)-Br(1)	80.5(2)
C(7)-S(1)-C(8)	104.0(3)
C(14)-S(2)-C(15)	103.7(4)
C(15)-S(2')-C(14)	99.6(5)
C(2)-N(1)-C(6)	118.6(6)
C(2)-N(1)-Pd(1)	120.9(5)
C(6)-N(1)-Pd(1)	119.7(4)
C(13)-N(2)-C(9)	119.6(7)
C(13)-N(2)-Pd(1)	120.5(5)
C(9)-N(2)-Pd(1)	119.2(5)
N(1)-C(2)-C(3)	121.2(8)
N(1)-C(2)-C(15)	117.6(7)
C(3)-C(2)-C(15)	121.3(7)
C(4)-C(3)-C(2)	119.8(7)
C(4)-C(3)-H(3)	120.1
C(2)-C(3)-H(3)	120.1
C(3)-C(4)-C(5)	120.1(8)
C(3)-C(4)-H(4)	120.0
C(5)-C(4)-H(4)	120.0
C(6)-C(5)-C(4)	118.2(8)
C(6)-C(5)-H(5)	120.9
C(4)-C(5)-H(5)	120.9
N(1)-C(6)-C(5)	122.0(6)
N(1)-C(6)-C(7)	117.4(6)
C(5)-C(6)-C(7)	120.6(7)

C(6)-C(7)-S(1)	115.9(4)
C(6)-C(7)-H(7A)	108.3
S(1)-C(7)-H(7A)	108.3
C(6)-C(7)-H(7B)	108.3
S(1)-C(7)-H(7B)	108.3
H(7A)-C(7)-H(7B)	107.4
C(9)-C(8)-S(1)	115.1(5)
C(9)-C(8)-H(8A)	108.5
S(1)-C(8)-H(8A)	108.5
C(9)-C(8)-H(8B)	108.5
S(1)-C(8)-H(8B)	108.5
H(8A)-C(8)-H(8B)	107.5
N(2)-C(9)-C(10)	121.5(7)
N(2)-C(9)-C(8)	118.4(6)
C(10)-C(9)-C(8)	120.1(7)
C(9)-C(10)-C(11)	118.6(8)
C(9)-C(10)-H(10)	120.7
C(11)-C(10)-H(10)	120.7
C(12)-C(11)-C(10)	118.5(8)
C(12)-C(11)-H(11)	120.8
C(10)-C(11)-H(11)	120.8
C(11)-C(12)-C(13)	120.9(8)
C(11)-C(12)-H(12)	119.6
C(13)-C(12)-H(12)	119.6
N(2)-C(13)-C(12)	120.8(8)
N(2)-C(13)-C(14)	118.1(8)
C(12)-C(13)-C(14)	121.0(7)
C(13)-C(14)-S(2)	123.1(7)
C(13)-C(14)-S(2')	105.4(7)
C(13)-C(14)-H(14A)	106.6
S(2)-C(14)-H(14A)	106.6
S(2')-C(14)-H(14A)	119.0
C(13)-C(14)-H(14B)	106.6
S(2)-C(14)-H(14B)	106.6
S(2')-C(14)-H(14B)	112.1

H(14A)-C(14)-H(14B)	106.5
C(2)-C(15)-S(2)	123.4(7)
C(2)-C(15)-S(2')	105.7(7)
C(2)-C(15)-H(15A)	106.5
S(2)-C(15)-H(15A)	106.5
S(2')-C(15)-H(15A)	111.9
C(2)-C(15)-H(15B)	106.5
S(2)-C(15)-H(15B)	106.5
S(2')-C(15)-H(15B)	119.1
H(15A)-C(15)-H(15B)	106.5
Pd(1)-C(1)-H(1A)	109.5
Pd(1)-C(1)-H(1B)	109.5
H(1A)-C(1)-H(1B)	109.5
Pd(1)-C(1)-H(1C)	109.5
H(1A)-C(1)-H(1C)	109.5
H(1B)-C(1)-H(1C)	109.5
Pd(1)-C(1')-H(1'A)	109.5
Pd(1)-C(1')-H(1'B)	109.5
H(1'A)-C(1')-H(1'B)	109.5
Pd(1)-C(1')-H(1'C)	109.5
H(1'A)-C(1')-H(1'C)	109.5
H(1'B)-C(1')-H(1'C)	109.5

Projection view with 30% thermal ellipsoids:

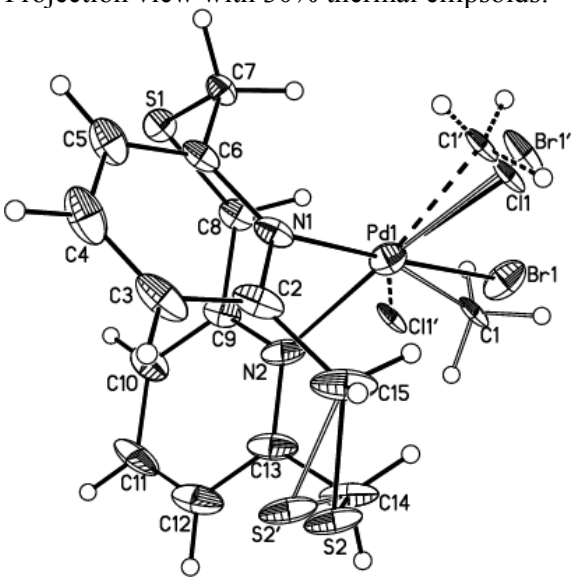

2) (N2S2-O)$Pd^{II}Cl_2$, **7** (lm9112).

Table 1. Crystal data and structure refinement for lm9112.

Identification code	l9112/lt/JL040212-A	
Empirical formula	$C_{28}H_{28}BCl_3F_4N_4O_{0.14}Pd_2S_4$	
Formula weight	956.94	
Temperature	100(2) K	
Wavelength	0.71073 Å	
Crystal system	Monoclinic	
Space group	$P2_1/c$	
Unit cell dimensions	a = 8.9480(12) Å	α= 90°.
	b = 15.529(2) Å	β= 98.914(7)°.
	c = 23.928(3) Å	γ = 90°.
Volume	3284.8(7) $Å^3$	
Z	4	
Density (calculated)	1.935 Mg/m^3	
Absorption coefficient	1.646 mm^{-1}	
F(000)	1892	
Crystal size	0.10 x 0.07 x 0.04 mm^3	
Theta range for data collection	1.72 to 24.00°.	
Index ranges	$-10 \le h \le 10$, $-16 \le k \le 17$, $-27 \le l \le 27$	
Reflections collected	54615	
Independent reflections	5151 [R(int) = 0.2444]	
Completeness to theta = 24.00°	100.0 %	
Absorption correction	Semi-empirical from equivalents	
Max. and min. transmission	0.9311 and 0.8501	
Refinement method	Full-matrix least-squares on F^2	
Data / restraints / parameters	5151 / 194 / 431	
Goodness-of-fit on F^2	1.002	
Final R indices [I>2sigma(I)]	R1 = 0.0574, wR2 = 0.1014	
R indices (all data)	R1 = 0.1409, wR2 = 0.1331	
Largest diff. peak and hole	0.903 and -0.938 $e.Å^{-3}$	

Table 2. Bond lengths [Å] and angles [°] for lm9112.

Pd(1)-N(1)	2.044(8)
Pd(1)-N(2)	2.046(8)
Pd(1)-Cl(1)	2.286(3)
Pd(1)-Cl(2)	2.289(3)
S(1)-O(1)	1.449(5)
S(1)-C(6)	1.805(11)
S(1)-C(7)	1.811(11)
S(2)-C(13)	1.809(11)
S(2)-C(14)	1.812(10)
N(1)-C(5)	1.352(12)
N(1)-C(1)	1.379(12)
N(2)-C(8)	1.360(13)
N(2)-C(12)	1.367(12)
C(1)-C(2)	1.357(14)
C(1)-C(14)	1.496(15)
C(2)-C(3)	1.380(15)
C(2)-H(2)	0.9500
C(3)-C(4)	1.393(14)
C(3)-H(3)	0.9500
C(4)-C(5)	1.391(13)
C(4)-H(4)	0.9500
C(5)-C(6)	1.499(14)
C(6)-H(6A)	0.9900
C(6)-H(6B)	0.9900
C(7)-C(8)	1.499(14)
C(7)-H(7A)	0.9900
C(7)-H(7B)	0.9900
C(8)-C(9)	1.375(14)
C(9)-C(10)	1.378(14)
C(9)-H(9)	0.9500
C(10)-C(11)	1.369(15)
C(10)-H(10)	0.9500
C(11)-C(12)	1.381(14)

C(11)-H(11)	0.9500
C(12)-C(13)	1.498(14)
C(13)-H(13A)	0.9900
C(13)-H(13B)	0.9900
C(14)-H(14A)	0.9900
C(14)-H(14B)	0.9900
Pd(2)-N(3)	2.014(8)
Pd(2)-Cl(3)	2.305(3)
Pd(2)-S(4)	2.308(3)
Pd(2)-S(3)	2.335(3)
Pd(2)-N(4)	2.543(8)
S(3)-C(20)	1.798(11)
S(3)-C(21)	1.845(10)
S(4)-C(28)	1.814(11)
S(4)-C(27)	1.848(10)
N(3)-C(15)	1.375(12)
N(3)-C(19)	1.379(12)
N(4)-C(26)	1.337(12)
N(4)-C(22)	1.342(12)
C(15)-C(16)	1.380(14)
C(15)-C(28)	1.478(14)
C(16)-C(17)	1.374(15)
C(16)-H(16)	0.9500
C(17)-C(18)	1.377(15)
C(17)-H(17)	0.9500
C(18)-C(19)	1.365(14)
C(18)-H(18)	0.9500
C(19)-C(20)	1.511(14)
C(20)-H(20A)	0.9900
C(20)-H(20B)	0.9900
C(21)-C(22)	1.531(13)
C(21)-H(21A)	0.9900
C(21)-H(21B)	0.9900
C(22)-C(23)	1.370(14)
C(23)-C(24)	1.366(14)

C(23)-H(23)	0.9500
C(24)-C(25)	1.384(14)
C(24)-H(24)	0.9500
C(25)-C(26)	1.382(14)
C(25)-H(25)	0.9500
C(26)-C(27)	1.488(13)
C(27)-H(27A)	0.9900
C(27)-H(27B)	0.9900
C(28)-H(28A)	0.9900
C(28)-H(28B)	0.9900
B(1)-F(4')	1.386(9)
B(1)-F(3)	1.387(7)
B(1)-F(1)	1.388(7)
B(1)-F(4)	1.398(7)
B(1)-F(2')	1.402(8)
B(1)-F(2)	1.409(7)
B(1)-F(3')	1.411(8)

N(1)-Pd(1)-N(2)	89.0(3)
N(1)-Pd(1)-Cl(1)	88.9(2)
N(2)-Pd(1)-Cl(1)	176.4(2)
N(1)-Pd(1)-Cl(2)	178.2(2)
N(2)-Pd(1)-Cl(2)	90.5(2)
Cl(1)-Pd(1)-Cl(2)	91.74(10)
O(1)-S(1)-C(6)	103(2)
O(1)-S(1)-C(7)	118(2)
C(6)-S(1)-C(7)	102.5(5)
C(13)-S(2)-C(14)	103.4(5)
C(5)-N(1)-C(1)	119.3(9)
C(5)-N(1)-Pd(1)	119.2(7)
C(1)-N(1)-Pd(1)	121.5(7)
C(8)-N(2)-C(12)	120.0(9)
C(8)-N(2)-Pd(1)	121.4(7)
C(12)-N(2)-Pd(1)	118.4(7)
C(2)-C(1)-N(1)	120.6(10)

C(2)-C(1)-C(14)	122.1(10)
N(1)-C(1)-C(14)	117.3(9)
C(1)-C(2)-C(3)	121.7(11)
C(1)-C(2)-H(2)	119.2
C(3)-C(2)-H(2)	119.2
C(2)-C(3)-C(4)	117.5(10)
C(2)-C(3)-H(3)	121.2
C(4)-C(3)-H(3)	121.2
C(5)-C(4)-C(3)	120.2(10)
C(5)-C(4)-H(4)	119.9
C(3)-C(4)-H(4)	119.9
N(1)-C(5)-C(4)	120.7(10)
N(1)-C(5)-C(6)	119.5(9)
C(4)-C(5)-C(6)	119.8(10)
C(5)-C(6)-S(1)	114.6(7)
C(5)-C(6)-H(6A)	108.6
S(1)-C(6)-H(6A)	108.6
C(5)-C(6)-H(6B)	108.6
S(1)-C(6)-H(6B)	108.6
H(6A)-C(6)-H(6B)	107.6
C(8)-C(7)-S(1)	115.6(7)
C(8)-C(7)-H(7A)	108.4
S(1)-C(7)-H(7A)	108.4
C(8)-C(7)-H(7B)	108.4
S(1)-C(7)-H(7B)	108.4
H(7A)-C(7)-H(7B)	107.4
N(2)-C(8)-C(9)	119.8(10)
N(2)-C(8)-C(7)	118.6(9)
C(9)-C(8)-C(7)	121.5(10)
C(8)-C(9)-C(10)	121.1(11)
C(8)-C(9)-H(9)	119.4
C(10)-C(9)-H(9)	119.4
C(11)-C(10)-C(9)	118.4(11)
C(11)-C(10)-H(10)	120.8
C(9)-C(10)-H(10)	120.8

C(10)-C(11)-C(12)	120.6(11)
C(10)-C(11)-H(11)	119.7
C(12)-C(11)-H(11)	119.7
N(2)-C(12)-C(11)	120.0(10)
N(2)-C(12)-C(13)	118.6(9)
C(11)-C(12)-C(13)	121.4(10)
C(12)-C(13)-S(2)	114.3(8)
C(12)-C(13)-H(13A)	108.7
S(2)-C(13)-H(13A)	108.7
C(12)-C(13)-H(13B)	108.7
S(2)-C(13)-H(13B)	108.7
H(13A)-C(13)-H(13B)	107.6
C(1)-C(14)-S(2)	115.9(7)
C(1)-C(14)-H(14A)	108.3
S(2)-C(14)-H(14A)	108.3
C(1)-C(14)-H(14B)	108.3
S(2)-C(14)-H(14B)	108.3
H(14A)-C(14)-H(14B)	107.4
N(3)-Pd(2)-Cl(3)	174.1(2)
N(3)-Pd(2)-S(4)	86.4(2)
Cl(3)-Pd(2)-S(4)	92.39(10)
N(3)-Pd(2)-S(3)	85.7(2)
Cl(3)-Pd(2)-S(3)	97.06(10)
S(4)-Pd(2)-S(3)	161.56(10)
N(3)-Pd(2)-N(4)	85.5(3)
Cl(3)-Pd(2)-N(4)	100.1(2)
S(4)-Pd(2)-N(4)	81.7(2)
S(3)-Pd(2)-N(4)	81.08(19)
C(20)-S(3)-C(21)	102.5(5)
C(20)-S(3)-Pd(2)	96.7(3)
C(21)-S(3)-Pd(2)	100.8(3)
C(28)-S(4)-C(27)	101.6(5)
C(28)-S(4)-Pd(2)	97.3(3)
C(27)-S(4)-Pd(2)	99.6(3)
C(15)-N(3)-C(19)	119.0(9)

C(15)-N(3)-Pd(2)	120.3(7)
C(19)-N(3)-Pd(2)	120.7(7)
C(26)-N(4)-C(22)	119.1(9)
C(26)-N(4)-Pd(2)	103.6(6)
C(22)-N(4)-Pd(2)	104.4(6)
N(3)-C(15)-C(16)	120.1(10)
N(3)-C(15)-C(28)	117.8(9)
C(16)-C(15)-C(28)	121.9(10)
C(17)-C(16)-C(15)	120.1(11)
C(17)-C(16)-H(16)	120.0
C(15)-C(16)-H(16)	120.0
C(16)-C(17)-C(18)	120.1(11)
C(16)-C(17)-H(17)	120.0
C(18)-C(17)-H(17)	120.0
C(19)-C(18)-C(17)	119.4(11)
C(19)-C(18)-H(18)	120.3
C(17)-C(18)-H(18)	120.3
C(18)-C(19)-N(3)	121.4(10)
C(18)-C(19)-C(20)	121.9(9)
N(3)-C(19)-C(20)	116.7(9)
C(19)-C(20)-S(3)	115.8(7)
C(19)-C(20)-H(20A)	108.3
S(3)-C(20)-H(20A)	108.3
C(19)-C(20)-H(20B)	108.3
S(3)-C(20)-H(20B)	108.3
H(20A)-C(20)-H(20B)	107.4
C(22)-C(21)-S(3)	113.4(7)
C(22)-C(21)-H(21A)	108.9
S(3)-C(21)-H(21A)	108.9
C(22)-C(21)-H(21B)	108.9
S(3)-C(21)-H(21B)	108.9
H(21A)-C(21)-H(21B)	107.7
N(4)-C(22)-C(23)	122.1(9)
N(4)-C(22)-C(21)	112.5(9)
C(23)-C(22)-C(21)	125.0(10)

C(24)-C(23)-C(22)	118.8(10)
C(24)-C(23)-H(23)	120.6
C(22)-C(23)-H(23)	120.6
C(23)-C(24)-C(25)	119.5(10)
C(23)-C(24)-H(24)	120.2
C(25)-C(24)-H(24)	120.2
C(26)-C(25)-C(24)	118.7(10)
C(26)-C(25)-H(25)	120.7
C(24)-C(25)-H(25)	120.7
N(4)-C(26)-C(25)	121.3(9)
N(4)-C(26)-C(27)	113.9(9)
C(25)-C(26)-C(27)	124.6(9)
C(26)-C(27)-S(4)	112.5(7)
C(26)-C(27)-H(27A)	109.1
S(4)-C(27)-H(27A)	109.1
C(26)-C(27)-H(27B)	109.1
S(4)-C(27)-H(27B)	109.1
H(27A)-C(27)-H(27B)	107.8
C(15)-C(28)-S(4)	116.4(7)
C(15)-C(28)-H(28A)	108.2
S(4)-C(28)-H(28A)	108.2
C(15)-C(28)-H(28B)	108.2
S(4)-C(28)-H(28B)	108.2
H(28A)-C(28)-H(28B)	107.4
F(4')-B(1)-F(3)	108.2(19)
F(4')-B(1)-F(1)	135.3(19)
F(3)-B(1)-F(1)	116.6(8)
F(4')-B(1)-F(4)	49.5(16)
F(3)-B(1)-F(4)	112.0(8)
F(1)-B(1)-F(4)	108.6(7)
F(4')-B(1)-F(2')	111.0(17)
F(3)-B(1)-F(2')	51.6(13)
F(1)-B(1)-F(2')	97.9(13)
F(4)-B(1)-F(2')	153.4(14)
F(4')-B(1)-F(2)	57.1(17)

F(3)-B(1)-F(2)	107.8(8)
F(1)-B(1)-F(2)	107.6(7)
F(4)-B(1)-F(2)	103.4(8)
F(2')-B(1)-F(2)	68.9(13)
F(4')-B(1)-F(3')	111.8(17)
F(3)-B(1)-F(3')	50.1(10)
F(1)-B(1)-F(3')	96.4(11)
F(4)-B(1)-F(3')	77.9(11)
F(2')-B(1)-F(3')	98.0(14)
F(2)-B(1)-F(3')	153.8(12)

Projection view with 50% thermal ellipsoids - O atom occupancy is 14%:

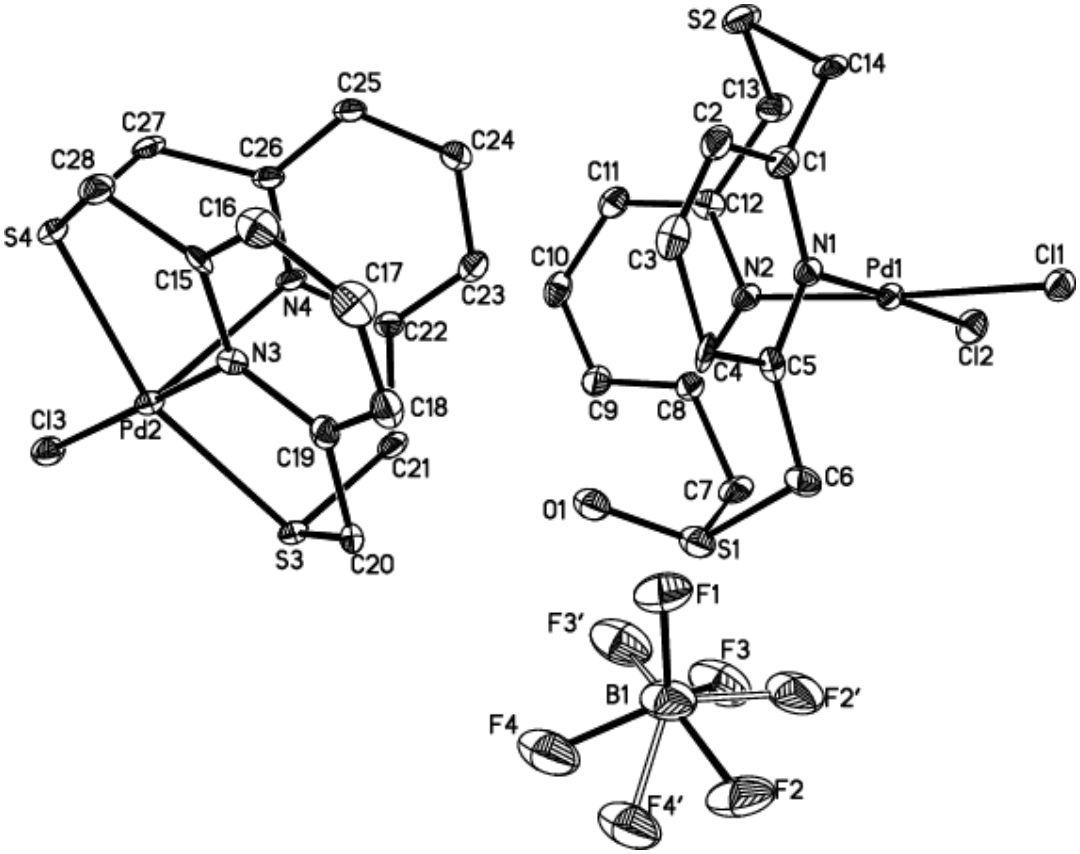

X. References

1. M. J. Frisch, G. W. T., H. B. Schlegel, G. E. Scuseria, M. A. Robb, J. R. Cheeseman, G. Scalmani, V. Barone, B. Mennucci, G. A. Petersson, H. Nakatsuji, M. Caricato, X. Li, H. P. Hratchian, A. F. Izmaylov, J. Bloino, G. Zheng, J. L. Sonnenberg, M. Hada, M. Ehara, K. Toyota, R. Fukuda, J. Hasegawa, M. Ishida, T. Nakajima, Y. Honda, O. Kitao, H. Nakai, T. Vreven, J. A. Montgomery, Jr., J. E. Peralta, F. Ogliaro, M. Bearpark, J. J. Heyd, E. Brothers, K. N. Kudin, V. N. Staroverov, R. Kobayashi, J. Normand, K. Raghavachari, A. Rendell, J. C. Burant, S. S. Iyengar, J. Tomasi, M. Cossi, N. Rega, J. M. Millam, M. Klene, J. E. Knox, J. B. Cross, V. Bakken, C. Adamo, J. Jaramillo, R. Gomperts, R. E. Stratmann, O. Yazyev, A. J. Austin, R. Cammi, C. Pomelli, J. W. Ochterski, R. L. Martin, K. Morokuma, V. G. Zakrzewski, G. A. Voth, P. Salvador, J. J. Dannenberg, S. Dapprich, A. D. Daniels, O. Farkas, J. B. Foresman, J. V. Ortiz, J. Cioslowski, D. J. Fox, *Gaussian 09, Revision A.02*, A.02; Gaussian, Inc.: Wallingford CT, 2009.

2. a) Becke, A. D., *J. Chem. Phys.* **1993,** *98*, 1372-1377. b) Lee, C. T.; Yang, W. T.; Parr, R. G., *Phys. Rev. B* **1988,** *37*, 785-789.

3. a) Stevens, W. J.; Basch, H.; Krauss, M., *J. Chem. Phys.* **1984,** *81*, 6026-6033. b) Stevens, W. J.; Krauss, M.; Basch, H.; Jasien, P. G., *Can. J. Chem.* **1992,** *70*, 612-630.

4. a) Foley, N. A.; Lail, M.; Lee, J. P.; Gunnoe, T. B.; Cundari, T. R.; Petersen, J. L., *J. Am. Chem. Soc.* **2007,** *129*, 6765-6781. b) Veige, A. S.; Slaughter, L. M.; Wolczanski, P. T.; Matsunaga, N.; Decker, S. A.; Cundari, T. R., *J. Am. Chem. Soc.* **2001,** *123*, 6419-6420.

5. Skripnikov, L. *Chemissian, version 1.771, 2010*, www.chemissian.com, accessed June 2011

6. O'Boyle, N. M.; Tenderholt, A. L.; Langner, K. M. *J. Comp. Chem.* **2008**, *29*, 839.